Molecular Biology of the Cell
Vol. 11, 3539–3558, October 2000

Coiled-Coil Trigger Motifs in the 1B and 2B Rod Domain Segments Are Required for the Stability of Keratin Intermediate Filaments

Kenneth C. Wu,* Janine T. Bryan,* Maria I. Morasso,* Shyh-Ing Jang,* Jeung-Hoon Lee,† Jun-Mo Yang,‡ Lyuben N. Marekov,* David A.D. Parry,§ and Peter M. Steinert*‖

*Laboratory of Skin Biology, National Institute of Arthritis and Musculoskeletal and Skin Diseases, National Institutes of Health, Bethesda, Maryland 20892; †Department of Dermatology, Chungnam National University Hospital, Tae-Jon, Republic of Korea; ‡Department of Dermatology, Sungkyunkwan University School of Medicine, Center for Clinical Research, Samsung Biomedical Research Institute, Seoul 135-710, Republic of Korea; and §Institute of Fundamental Sciences, Massey University, Palmerston North, New Zealand

Submitted January 28, 2000; Revised July 10, 2000; Accepted July 17, 2000
Monitoring Editor: Paul T. Matsudaira

Many α-helical proteins that form two-chain coiled coils possess a 13-residue trigger motif that seems to be required for the stability of the coiled coil. However, as currently defined, the motif is absent from intermediate filament (IF) protein chains, which nevertheless form segmented two-chain coiled coils. In the present work, we have searched for and identified two regions in IF chains that are essential for the stability necessary for the formation of coiled-coil molecules and thus may function as trigger motifs. We made a series of point substitutions with the keratin 5/keratin 14 IF system. Combinations of the wild-type and mutant chains were assembled in vitro and in vivo, and the stabilities of two-chain (one-molecule) and two-molecule assemblies were examined with use of a urea disassembly assay. Our new data document that there is a region located between residues 100 and 113 of the 2B rod domain segment that is absolutely required for molecular stability and IF assembly. This potential trigger motif differs slightly from the consensus in having an Asp residue at position 4 (instead of a Glu) and a Thr residue at position 9 (instead of a charged residue), but there is an absolute requirement for a Glu residue at position 6. Because these 13 residues are highly conserved, it seems possible that this motif functions in all IF chains. Likewise, by testing keratin IF with substitutions in both chains, we identified a second potential trigger motif between residues 79 and 91 of the 1B rod domain segment, which may also be conserved in all IF chains. However, we were unable to find a trigger motif in the 1A rod domain segment. In addition, many other point substitutions had little detectable effect on IF assembly, except for the conserved Lys-23 residue of the 2B rod domain segment. Cross-linking and modeling studies revealed that Lys-23 may lie very close to Glu-106 when two molecules are aligned in the A_{22} mode. Thus, the Glu-106 residue may have a dual role in IF structure: it may participate in trigger formation to afford special stability to the two-chain coiled-coil molecule, and it may participate in stabilization of the two-molecule hierarchical stage of IF structure.

INTRODUCTION

Intermediate filaments (IF) are ubiquitous constituents of the cytoskeletons of eukaryotic cells. Much is now known about their expression characteristics in cells. Recent evidence, largely based on naturally occurring mutations in human diseases or experimental knockout experiments in transgenic mice, have provided a wealth of information on their possible or likely structural functions in many cell types (Fuchs and Weber, 1994; Parry and Steinert, 1995, 1999; Irvine and McLean, 1999). In addition, cell biological experiments have elegantly documented that IF are highly dynamic, continually exchanging protein along their length

‖ Corresponding author. E-mail address: pemast@helix.nih.gov.
Abbreviations used: DST, disulfosuccinimyd l tartrate; GFP, green fluorescent protein; IF, intermediate filaments; KX, keratin X, as in K5 for the keratin 5 chain.

and changing their supramolecular organization in living cells (Yoon *et al.*, 1998). Together, these data suggest that IF subserve a dynamic structural role in the maintenance of cell shape and function and directly affect the biomechanical properties of an entire tissue, especially epithelia.

In contrast, rather less is known about structure. However, it is now appreciated that IF structure can be evaluated through several hierarchical levels of increasing order, although regrettably with a declining level of confidence with increasing degrees of complexity (for reviews, see Parry and Steinert, 1995, 1999; Herrmann and Aebi, 1998). All IF chains contain a central rod domain composed of four α-helical segments of conserved size that possess a repeating heptad sequence motif, interspersed with flexible linker sequences, and flanked on the amino and carboxyl termini by head and tail domains. Based largely on sequence homologies, six distinct classes of IF chains have been identified, each containing multiple members.

The initial step in IF assembly is the formation of a two-chain molecule by the parallel in-register alignment of two compatible IF protein chains in which the aligned α-helical segments form coiled coils, resulting in a structure that is 45–47 nm long (for reviews, see Parry and Steinert, 1995, 1999; Herrmann and Aebi, 1998, 1999). Although the details of the compatibility of the two chains remain poorly defined, the molecule is known to be stabilized in large part by interactions of hydrophobic residues in the *a* and *d* heptad positions, which form a "knob-in-hole" backbone for the coiled coil. Considerable speculation has suggested that the formation of ionic salt bonds between oppositely charged residues might also be important in molecular stabilization (Cohen and Parry, 1990, 1994). Theoretically, such bonds could be intrachain, involving $i,i + 4$ interactions between oppositely charged residues three or four residues apart on the same chain (Letai and Fuchs, 1995), or they could be intermolecular, arising from oppositely charged residues occupying primarily the *e* and *g* positions across the two chains, defined as a $1e - 2g'$ interaction. However, detailed studies of model systems have demonstrated that $1e - 2g'$ interactions do not stabilize coiled coils (O'Shea *et al.*, 1992, 1993a,b; Harbury *et al.*, 1994; Lavigne and Kim, 1995; Yu *et al.*, 1996) but might control coiled-coil specificity and oligomerization state instead (Krylov *et al.*, 1994; Zhou *et al.*, 1994; Lumb and Kim, 1995; Kohn *et al.*, 1998).

Recent evidence has indicated that many proteins that form two-chain coiled coils possess a 13-residue "trigger" motif that seems to confer special stability for the formation of a coiled coil (Kammerer *et al.*, 1998; Steinmetz *et al.*, 1998). Notably, however, the motif as currently defined is absent in all IF chains examined, but regions of some similarity occur toward the ends of the 1A, 1B, and 2B rod domain segments (Table 1). Thus, it remains to be established whether these or other regions function as stabilizing trigger motifs in IF coiled coils.

The next level of IF structural hierarchy is the tetramer, formed by the antiparallel alignment of two molecules in one of three basic modes, termed A_{11}, A_{22}, and A_{12}, based on which portions of the rod domains partially or fully overlap (Heins *et al.*, 1993; Steinert *et al.*, 1993a,b,c; Parry and Steinert, 1995, 1999). The A_{11} and A_{22} alignments produce particles 60–70 nm long that are fully compatible with assembly into IF in vitro. At protein concentrations less than the critical concentration required for IF assembly (~40 μg/ml) and at pH values between 6.5 and 8, most IF types exist in solution largely as tetramers that presumably consist of mixtures of these two modes (although larger oligomers may also be present, depending on the exact buffer and assembly conditions used). We have shown that tetramers in the fully overlapped antiparallel A_{12} alignment are stable only at high pH values, under which conditions IF assembly does not occur, so they are assembly incompetent, although when the pH is decreased the two molecules rearrange by "tetramer switching" to the A_{11} or A_{22} mode (Steinert, 1991). Interestingly, the exact molecule alignments in the A_{11} and A_{22} modes differ between the various types of IF (Steinert *et al.*, 1993c, 1999). However, fundamental questions regarding how the A_{11} and A_{22} modes are stabilized remain poorly understood. Examination of the first few seconds of IF assembly in vitro has revealed the formation of "unit-length" particles that are 70 nm long, which later elongate into typical IF structures (Herrmann *et al.*, 1999, 2000, and references therein). These particles are commonly 8–16 molecules wide (although wider structures may be formed, depending on the assembly conditions used) and, based on our earlier analyses, presumably consist of a stacked array of alternating rows of A_{11} and A_{12} or A_{22} and A_{12} molecules (Herrmann and Aebi, 1999).

We have been intrigued by the occurrence of an apparent conservative glutamic acid-to-aspartic acid substitution in the 2B rod domain segment (Glu106Asp) of the keratin 1 chain in a case of moderately severe epidermolytic hyperkeratosis (Yang *et al.*, 1999). Because this residue is located near the center of a candidate trigger-like motif of the 2B rod domain segment (Table 1), in this study we have explored in more detail the roles of charged residues in the molecular and tetramer stability of IF. With the use of point mutations in the keratin 5/keratin 14 (K5/K14) system, our new data suggest that there is indeed a region in each of the 1B and 2B segments that is essential for the stability of coiled coils and thus may serve as trigger motifs. Furthermore, we show that Glu-106 of the 2B segment is important for stabilizing the A_{22} mode of alignment of two neighboring molecules within IF.

MATERIALS AND METHODS

Preparation of Wild-Type and Mutant K5 and K14 Chains

Full-length human K5 and K14 cDNAs were assembled into a pET11a vector for expression in bacteria as described previously (Candi *et al.*, 1998). A series of mutant forms of both chains were generated with the use of the QuickChange site-directed mutagenesis kit (Stratagene, La Jolla, CA) (Table 2). DNA sequencing was done to proofread and confirm the mutations. After induction, inclusion bodies were recovered, dissolved in SDS-PAGE buffer, and resolved in 3-mm-thick slab gels. The desired keratin bands were cut out and eluted into SDS gel buffer overnight, and the solutions were stored at −70°C.

In Vitro IF Assembly

Equimolar mixtures of either wild-type or mutant K5 and K14 chains were made from the stored SDS gel buffer solutions. The SDS was removed by ion-pair extraction (Konigsberg and Henderson, 1983), and the pelleted proteins were redissolved (0.05 or 0.5 mg/ml) in a buffer of 9.5 M urea containing 50 mM Tris-HCl (pH 7.6), 1 mM DTT, and 1 mM EDTA. IF were then assembled

Table 1. Potential trigger sequences in human IF protein chains: potential ionic charge interactions

Protein	Sequence																	Number of mismatches
Heptad position	*f*	*g*	*a*	*b*	*c*	*d*	*e*	*f*	*g*	*a*	*b*	*c*	*d*	*e*	*f*	*g*	*a*	*b*	
Trigger motif*	.	.	.	x	x	L	E	x	c	h	x	c	x	c	c	x	.	.	
Tropomyosin	R	S	V	T	K	L	E	K	E	I	D	D	L	E	D	E	L	Y	
Keratin 14 1A 16-31	D	K	V	R	A	L	E	E	A	N	A	D	L	E	V	K	I	R	3
Keratin 5 1A 16-31	D	K	V	R	F	L	E	Q	Q	N	K	V	L	E	T	K	W	T	4
Vimentin 1A 16-31	D	K	V	R	F	L	E	Q	Q	N	K	I	L	L	A	E	L	E	5
NF-L 1A 16-31	E	R	V	H	E	L	E	Q	Q	N	K	V	L	E	A	E	L	L	4
Lamin A 1A 16-31	D	R	V	R	S	L	E	T	E	N	A	G	L	R	L	R	I	T	3
Nestin 1A 16-31	G	R	V	K	A	L	E	E	Q	N	E	L	L	S	A	G	G	L	4
Keratin 14 1B 69-86	L	A	R	A	D	L	E	M	Q	I	E	S	L	K	E	E	L	A	2
Keratin 5 1B 69-86	M	N	K	V	E	L	R	A	K	V	D	A	L	M	D	E	I	N	2
Vimentin 1B 69-86	L	A	R	L	D	L	E	R	K	V	E	S	L	Q	E	E	I	A	2
NF-L 1B 69-86	L	A	R	A	E	L	E	K	R	I	D	S	L	M	D	E	I	A	2
Lamin A 1B 111-128	L	R	R	V	D	A	E	H	R	L	Q	T	M	K	E	E	L	D	2
Nestin 1B 69-86	C	A	R	A	W	L	S	S	Q	G	A	E	L	E	R	E	L	E	3
Keratin 14 1B 76-93	M	Q	I	E	S	L	K	E	E	L	A	Y	L	K	K	N	H	E	2
Keratin 5 1B 76-93	A	K	V	D	A	L	M	D	E	I	N	F	M	K	M	F	F	D	3
Vimentin 1B 76-93	R	K	V	E	S	L	Q	E	E	I	A	F	L	K	K	L	H	D	2
NF-L 1B 76-93	K	R	I	D	S	L	M	D	E	I	A	F	L	K	K	V	H	D	2
Lamin A 1B 118-135	H	R	L	Q	T	M	K	E	E	L	D	F	Q	K	N	I	Y	S	4
Nestin 1B 76-93	S	Q	G	A	E	L	E	R	E	L	E	A	L	R	V	A	H	E	2
Keratin 14 2B 98-115	D	V	K	T	R	L	E	Q	E	I	A	T	Y	R	R	L	L	E	1
Keratin 5 2B 98-115	N	T	K	A	L	L	D	V	E	I	A	T	Y	R	K	L	L	E	2
Vimentin 2B 98-115	N	V	K	L	A	L	D	V	E	I	A	T	Y	R	K	L	L	E	2
NF-L 2B 98-115	N	V	K	M	A	L	D	M	E	I	A	A	Y	R	K	L	L	E	2
Lamin A 2B 98-115	D	I	K	L	A	L	D	M	E	I	H	A	Y	R	K	L	L	E	2
Nestin 2B 98-115	H	L	K	M	S	L	D	L	E	V	A	T	Y	R	T	L	L	E	3

Residues identified in the 2B rod domain segment that are theoretically well positioned to form interchain and intrachain ionic interactions (Herrmann *et al.*, 2000) are shown in red and blue, respectively. Underlined residues are deviations from the consensus motif (Kammerer *et al.*, 1999).

by dialysis through solutions of decreasing urea into assembly buffer of 10 mM Tris-HCl (pH 7.6), 1 mM DTT, and 1 mM EDTA (Candi *et al.*, 1998). Final protein concentrations were 35–40 μg/ml, which is less than the critical concentration for assembly (Steinert, 1991), which results in only one to four molecule assemblies being formed, or 400 μg/ml for optimal IF assembly.Particles were examined by electron microscopy after negative staining with 0.2–0.7% uranyl acetate. Lengths of IF were measured as described previously (Steinert *et al.*, 1976) in fields of $\geq$400 μm^2.

Transfection Experiments with K14–Green Fluorescent Protein Plasmids

A chimeric construct, assembled by attaching at the 5′ end of the full-length coding sequence of wild-type K14 sequences encoding the green fluorescent protein (GFP), was a generous gift of Dr. R.D. Goldman (Northwestern University Medical School, Chicago, IL). Point mutations were made in the plasmid as described above.

PtK2 (NBL-5) cells, epithelium-like rat kangaroo kidney cells, were obtained from the American Type Culture Collection (Rockville, MD;

Table 2. Oligonucleotide primers used for K5 and K14 chain mutants

Construct	Oligonucleotide primers	pET11a	pEGFPK14-C1
Keratin 14			
1A Lys01Met	5′-CTG GTG GGC AGT GAG A**t**G GTG ACC ATG CAG AAC CTC-3′	X	
	3′-GAC CAC CCG TCA CTC T**a**C CCA TGG TAC GTC TTG GAG-5′		
1A Arg10Leu	5′-CAG AAC CTC AAT GAC C**t**C CTG GCC TCC TAC CTG GAC-3′		
	3′-GTC TTG GAG TTA CTG G**a**G GAC CGG AGG ATG GAC CTG-5′	X	
1A Lys17Met	5′-CCT CCT ACC TGG ACA **t**GG TGC GTG CTC TGG AGG AGG-3′	X	
	3′-GGA GGA TGG ACC TGT **a**CC ACG CAC GAG ACC TCC TCC-5		
1A Arg19Leu	5′-TAC CTG GAC AAG GTG C**t**T GCT CTG GAG GAG GCC-3′	X	
	3′-ATG GAC CTG TTC CAC G**a**A CGA GAC CTC CTC CGG-5′		
1A Glu22Asp	5′-GGT GCG TGC TCT GGA **c**GA GGC CAA CGC CGA CCT GG-3′	X	X
	3′-CCA GCG ACG AGA CCT **g**CT CCG GTT GCG GCT GGA CC-5′		
1A Glu22Ala	5′-GGT GCG TGC TCT GG**c** AGA GGC CAA CGC CGA CCT GG-3′	X	X
	3′-CCA GCG ACG AGA CC**g** TCT CCG GTT GCG GCT GGA CC-5′		
1B Arg12Met	5′-ACC ATT GAG GAC CTG A**t**G GAA CAA GAT TCT CAC AG-3′	X	
	3′-TGG TAA CTC CTG GAC T**a**C CTT GTT CTA AGA GTG TC-5′		
1B Asp56Glu	5′-CGC ATG AGT GTG GAA GCC GA**a** ATC AAT GGC CTG CGC AGG GT-3′		X
	3′-GCG TAC TCA CAC CTT CGG CT**t** TAG TTA CCG GAC GCG TCC CA-5′		
1B Asp56Ala	5′-CGC ATG AGT GTG GAA GCC G**c**C ATC AAT GGC CTG CGC AGG GT-3′		X
	3′-GCG TAC TCA CAC CTT CGG C**g**G TAG TTA CCG GAC GCG TCC CA-5′		
1B Glu75Ala	5′-TGG CCA GAG CTG ACC TGG **c**GA TGC AGA TTG AGA GCC TGA-3′	X	
	3′-ACC GGT CTC GAC TGG ACC **g**CT ACG TCT AAC TCT CGG ACT-5′		
1B Glu79Ala	5′-TGG AGA TGC AGA TTG **c**GA GCC TGA AGG AGG AGC TGG-3′		
	3′-ACC TCT ACG TCT AAC **g**CT CGG ACT TCC TCC TCG ACC-5′	X	
1B Lys82Glu	5′-ATG CAG ATT GAG AGC CTG **g**AG GAG GAG CTG GCC TAC CTG-3′	X	
	3′-TAC GTC TAA CTC TCG GAC **c**TC CTC CTC GAC CGG ATG GAC-5		
1B Glu84Asp	5′-GAG AGC CTG AAG GAG GA**c** CTG GCC TAC CTG AAG AAG AAC C-3′	X	X
	3′-CTC TCG GAC TTC CTC CT**g** GAC CGG ATG GAC TTC TTC TTG G-5′		
1B Glu84Lys	5′-GAG AGC CTG AAG GAG **a**AA CTG GCC TAC CTG AAG AAG AAC C-3′		X
	3′-CTC TCG GAC TTC CTC **t**TT GAC CGG ATG GAC TTC TTC TTG G-5′		
2B Lys04Met	5′-GAA TGG CTC TTC ACC A**t**G ACA GAG GAG CTG AAC CGC GA-3′	X	
	3′-CTT ACC GAG AAG TGG T**a**C TGT CTC CTC GAC TTG GCG CT-5′		
2B Lys23Ile	5′-CTG GTG CAG AGC GCC A**tt** AGC GAG ATC TCG GAG CTC CGG-3′	X	X
	3′-GAC CAC GTC TCG CCG T**aa** TCG CTC TAG AGC CTC GAG GCC-5′		
2B Glu39Asp	5′-CCA TGC AGA ACC TGG AGA TTG A**c**C TGC AGT CCC AGC TCA GCA-3′	X	
	3′-GGT ACG TCT TGG ACC TCT AAC T**g**G ACG TCA GGG TCG AGT CGT-5′		
2B Glu39Ala	5′-CCA TGC AGA ACC TGG AGA TTG **c**GC TGC AGT CCC AGC TCA GCA-3′	X	X
	3′-GGT ACG TCT TGG ACC TCT AAC **g**CG ACG TCA GGG TCG AGT CGT-5′		
2B Glu39Lys	5′-CCA TGC AGA ACC TGG AGA TT**a** AGC TGC AGT CCC AGC TCA GCA-3′	X	
	3′-GGT ACG TCT TGG ACC TCT AA**t** TCG ACG TCA GGG TCG AGT CGT-5′		
2B Glu76Ala	5′-GAG ATG ATT GGC AGC GTG G**c**G GAG CAG CTG GCC CAG CTC C-3′	X	
	3′-CTC TAC TAA CCG TCG CAC C**g**C CTC GTC GAC CGG GTC GAC G-5′		
2B Lys100Met	5′-CAG GAG CTC ATG AAC ACC A**t**G CTG GCC CTG GAC GTG GAG-3′	X	
	3′-GTC CTC GAG TAC TTG TGG T**a**C GAC CGG GAC CTG CAC CTC-5′		
2B Glu104Ala	5′-GGA CGT GAA GAC GCG GCT GG**c** GCA GGA GAT CGC CAC CTA CCG-3′	X	X
	3′-CCT GCA CTT CTG CGC CGA CC**g** CGT CCT CTG GCG GTG GAC GGC-5′		
2B Glu104Asp	5′-GGA CGT GAA GAC GCG GCT GGA **c**CA GGA GAT CGC CAC CTA CCG-3′	X	
	5′-CCT GCA CTT CTG CGC CGA CCT **g**GT CCT CTG GCG GTG GAT GGC-5′		
2B Glu106Asp	5′-CGC GGC TGG AGC AGG A**c**A TCG CCA CCT ACC GCC GCC-3′	X	X
	3′-GCG CCG ACC TCG TCC T**g**T AGC GGT GGA TGG CGG CGG-5′		
2B Glu106Ala	5′-CGC GGC TGG AGC AGG **c**GA TCG CCA CCT AGG GCC GCC-3′		X
	3′-GCG CCG ACC TCG TCC **g**CT AGC GGT GGA TGG CGG CGG-5′		
2B Glu106Lys	5′-CGC GGC TGG AGC AG**a** AGA TCG CCA CCT AGG GCC GCC-3′	X	X
	3′-GCG CCG ACC TCG TC**t** TCT AGC GGT GGA TGG CGG CGG-5′		
2B Thr109Asp	5′-CTG GAG CAG GAG ATC GCC **ga**C TAC CGC CGC CTG CTG GAG GAG-3′	X	
	3′-GAC CTC GTC CTC TAG CGG **ct**G ATG GCG GCG GAC GAC CTC CTC-5′		
2B Thr109Phe	5′-CTG GAG CAG GAG ATC GCC **tt**C TAC CGC CGC CTG CTG GAG GAG-3′	X	
	3′-GAC CTC GTC CTC TAG CGG **aa**G ATG GCG GCG GAC GAC CTC CTC-5′		
2B Thr109Lys	5′-CTG GAG CAG GAG ATC GCC **aaa** TAC CGC CGC CTG CTG GAG GAG-3′	X	
	3′-GAC CTC GTC CTC TAG CGG **ttt** ATG GCG CGC CTG GAC CTC CTC-5′		
2B Arg111Leu	5′-CAG GAG ATC GCC ACC TAC C**t**C CGC CTG CTG GAG GGC CGA-3′	X	X
	3′-GTC CTC TAG CGG TGG ATG G**a**G GCG GAC GAC CTC CCG GCT-5′		

(continued)

Table 2. (Continued)

Construct	Oligonucleotide primers	pET11a	pEGFPK14-C1
Keratin 5			
1A Lys17Met	5′-TGG AGC AGC AGA ACA **t**GG TTC TGG ACA CCA AGT GGA CC-3′	X	
	3′-ACC TCG TCG TCT TGT **a**CC AAG ACC TGT GGT TCA CCT GG-5′		
1A Glu22Asp	5′-GGT GCG GTT CCT GGA **c**CA GCA GAA CAA GGT TCT GG-3′	X	
	3′-CCA CGC CAA GGA CCT **g**GT CGT CTT GTT CCA AGA CC-5′		
1A Glu22Ala	5′-GGT GCG GTT CCT GG**c** GCA GCA GAA CAA GGT TCT GG-3′	X	
	3′-CCA CGC CAA GGA CC**g** CGT CGT CTT GTT CCA AGA CC-5′		
1B Glu54Ala	5′-AAG CGT ACC ACT GCT G**c**G AAT GAG TTT GTG ATG CTG-3′	X	
	3′-TTC GCA TGG TGA CGA C**g**C TTA CTC AAA CAC TAC GAC-5′		
1B Lys71Ile	5′-GCT GCC TAC ATG AAC A**t**A GTG GAG CTG GAG GCC AA-3′	X	
	3′-CGA CGG ATG TAC TTG T**a**T CAC CTC GAC CTC CGG TT-5′		
1B Asp79Ala	5′-CTG GAG GCC AAG GTT G**c**T GCA CTG ATG GAT GAG ATT-3′	X	
	3′-GAC CTC CGG TTC CAA C**g**A CGT GAC TAC CTA CTC TAA-5′		
1B Glu84Asp	5′-GCA CTG ATG GAT GA**c** ATT AAC TTC ATG AAG ATG TTC-3′	X	
	3′-CGT GAC TAC CTA CT**g** TAA TTG AAG TAC TTC TAC AAG-5′		
1B Glu84Ala	5′-GCA CTG ATG GAT G**c**G ATT AAC TTC ATG AAG ATG TTC-3′	X	
	3′-CGT GAC TAC CTA C**g**C TAA TTG AAG TAC TTC TAC AAG-5′		
1B Lys89Met	5′-GAG ATT AAC TTC ATG A**t**G ATG TTC CTT GAT GCG GAG CTG-3′	X	
	3′-CTC TAA TTG AAG TAC T**a**C TAC AAG GAA CTA CGC CTC GAC-5′		
2B Asp18Glu	5′-GAG ATT AAC TTC ATG AAG A**a**G TTC CTT GAT GCG GAG CTG-3′	X	
	3′-CTC TAA TTG AAG TAC TTC T**t**C AAG GAA CTA CGC CTC GAC-5′		
2B Asp18Ala	5′-CTG GCC GGC ATG GCG ATG **c**CC TCC GCA ACA CCA AGC-3′	X	
	3′-GAC CGG CCG TAC CGC TAC **g**GG AGG CGT TGT GGT TCG-5′		
2B Arg20Leu	5′-GGC ATG GCG ATG ACC TCC **t**CA ACA CCA AGC ATG AGA-3′	X	
	3′-CCG TAC CGC TAC TGG AGG **a**GT TGT GGT TCG TAC TCT-5′		
2B Lys23Ile	5′-GAT GAC CTC CGC AAC ACC A**tc** CAT GAG ATC ACA GAG ATG-3′	X	
	3′-CTA CTG GAG GCG TTG TGG T**ag** GTA CTC TAC TGT CTC TAC-5′		
2B Glu25Lys	5′-GAC CTC CGC AAC ACC AAG CAT **a**AG ATC ACA GAG ATG AAC-3′	X	
	3′-CTG GAG GCG TTG TGG TTC GTA **t**TC TAG TGT CTC TAC TTG-5′		
2B Glu25Ala	5′-GAC CTC CGC AAC ACC AAG CAT G**c**G ATC ACA GAG ATG AAC-3′	X	
	3′-CTG GAG GCG TTG TGG TTC GTA C**g**C TAG TGT CTC TAC TTG-5′		
2B Lys44Glu	5′-GCC GAG ATT GAC AAT GTC **g**AG AAA CAG TGC GCC AAT CTG-3′	X	
	3′-CGG CTC TAA CTG TTA CAG **c**TC TTT GTC ACG CGG TTA GAC-5′		
2B Asp104Glu	5′-CAC CCA GCT GGC CCT GGA **a**GT GGA GAT CGC CAC TTA CCG-3′	X	
	3′-GTG GGT CGA CCG GGA CCT **t**CA CCT CTA GCG GTG AAT GGC-5′		
2B Asp104Ala	5′-CAC CCA GCT GGC CCT GG**c** AGT GGA GAT CGC CAC TTA CCG-3′	X	
	3′-GTG GGT CGA CCG GGA CC**g** TCA CCT CTA GCG GTG AAT GGC-5′		
2B Asp104Lys	5′-CAC CCA GCT GGC CCT G**aa** AGT GGA GAT CGC CAC TTA CCG-3′	X	
	3′-GTG GGT CGA CCG GGA C**tt** TCA CCT CTA GCG GTG AAT GGC-5′		
2B Glu106Asp	5′-GGC CCT GGA CGT GGA **c**AT CGC CAC TTA CCG CAA GCT-3′	X	
	3′-CCG GGA CCT GCA CCT **g**TA GCG GTG AAT GGC GTT CGA-5′		
2B Glu106Ala	5′-GGC CCT GGA CGT GG**c** GAT CGC CAC TTA CCG CAA GCT-3′	X	
	3′-CCG GGA CCT GCA CC**g** CTA GCG GTG AAT GGC GTT CGA-5′		
2B Arg111Asp	5′-ATC GCC ACT TAC **ga**C AAG CTG CTG GAG GGC GAG-3′	X	
	3′-TAG CGG TGA ATG **ct**G TTC GAC GAC CTC CCG CTC-5′		
2B Arg111Leu	5′-ATC GCC ACT TAC C**t**C AAG CTG CTG GAG GGC GAG-3′	X	
	3′-TAG CGG TGA ATG G**a**G TTC GAC GAC CTC CCG CTC-5′		

number CCL-56). The cells were grown in 25-cm^2 tissue culture flasks and maintained in MEM (Eagle's minimal essential medium with nonessential amino acids, Earle's salts, and reduced sodium bicarbonate at 0.85 g/L) (Life Technologies, Grand Island, NY) plus 10% FBS. For cell passage at near confluence, the medium was aspirated, the cells were washed once with PBS, and 0.25% trypsin was applied for 20 s. The trypsin was aspirated, and the flask was allowed to stand at room temperature for 3 min. Five milliliters of medium was pipetted over the cells to dislodge them from the flask, and the cells were transferred to a 15-ml conical tube. After centrifugation (5 min at 1000 rpm) to pellet the cells, the medium was aspirated and the cells were resuspended in 2 ml of medium and counted.

For direct immunofluorescence studies, 3×10^5 cells/ml were plated in 35-mm sterile tissue culture dishes, each containing a glass coverslip. After 24 h, the cells were transfected with 1 μg of plasmid DNA per coverslip with 3 μg of Lipofectin as described by the manufacturer (Life Technologies). After 4 h, the mixture was aspirated, and 1 ml of 15% glycerol in keratinocyte-serum free medium (Life Technologies) was applied for 3.5 min. The glycerol solution was replaced with 2 ml of fresh medium, and the cells were incubated at 37°C with 5% CO_2 for at least 24 h. The coverslips were recovered, washed in PBS, and mounted onto glass slides with Gel/Mount (Biomeda, Foster City, CA). Intracellular localization of GFP fusion proteins was determined by direct fluorescence microscopy.

Protein Chemistry Procedures

All protein concentrations were determined by amino acid analysis after acid hydrolysis. To examine molecular stabilities, equimolar mixtures of the desired K5/K14 chains (50 μg/ml) were equilibrated by a 2-h dialysis into urea solutions of the required concentration in a buffer of 10 mM triethanolamine (pH 8.0). The proteins were then cross-linked by reaction with 25 mM disulfosuccinimydl tartrate (DST) for 1 h at 23°C and terminated with 0.1 M NH_4HCO_3 (final concentration) as described previously (Steinert *et al.*, 1999). In these conditions, virtually all lysine residues are quantitatively modified by attachment of one side of the bifunctional cross-linker, but significant cross-linking between adjacent lysines also occurred. Products were examined by PAGE on 3.75–7.5% gradient gels.

To assess molecular alignments in the A_{11} and A_{22} modes, cross-linking with DST was performed with the use of 0.4 mM reagent exactly as described previously (Steinert *et al.*, 1993a,b). We used wild-type and mutant proteins that had been equilibrated into assembly buffer at ~40 μg/ml for 1–8 h. In this case, <10% of the lysine residues were chemically modified, except for several apparently fortuitously aligned residues that formed cross-links with yields of up to ~0.3 mol/mol. After cleavage with cyanogen bromide and trypsin digestion, peptides were resolved by HPLC as described previously. The positions of elution of the peptides cross-linked by DST corresponding to the A_{11} and A_{22} molecular alignment modes were similar to those published previously (Steinert *et al.*, 1993b). Semiquantitative estimates of the molar yields of each peptide were made based on peak heights of the integrated HPLC profiles.

Solutions of IF particles formed at 40 μg/ml were chromatographed by fast-performance liquid chromatography at 1 ml/min on a 25 × 1.1 cm column of Sepharose CL-400 equilibrated in IF assembly buffer (Steinert, 1991). In tetramer switching experiments, IF were mixed with an equal volume of a solution containing 50 mM sodium phosphate (pH 9.8), 1 mM DTT, and 1 mM EDTA, reacted at 23°C for 2 h, and chromatographed on the same column equilibrated in a buffer containing 25 mM sodium phosphate (pH 9.8), 1 mM DTT, and 1 mM EDTA. In some experiments, the samples were chromatographed within 1–60 min of the buffer change.

RESULTS

Detailed searches along the rod domain segments of IF chains revealed only four regions (Table 1) that display reasonable homology to the trigger motif reported in other coiled-coil proteins (Kammerer *et al.*, 1998). The possible roles of these regions in stabilizing IF coiled coils and in trigger motifs were explored in detail with the use of mutant chains carrying point substitutions. We used the K5/K14 IF system. The mutants used are listed in Table 2. We performed three types of experiments to explore the following: 1) the propensity of various equimolar mixtures of wild-type and mutant chains for keratin IF assembly in vitro, with the following criteria: the formation (or not) of recognizable IF structures, length, and gross morphology (Figure 2; Table 3); 2) the capacities of GFP-tagged K14 constructs with some identical substitutions to participate in IF assembly when transfected into PtK2 epithelial cells (Figure 3; Table 3); and 3) the comparative stabilities in concentrated urea solutions of one-molecule and two-molecule (tetramer) particles assembled from the wild-type and mutant chains (Figure 4; Table 4).

The Conserved Residue Glu-106 of the 2B Rod Domain Segment Is Required for IF Assembly

In initial experiments, we chose to mutate a variety of charged residues along the rod domain segments. Although there are many charged residues in K5 and K14, we note in particular that several positions are always occupied by either an acidic or a basic residue in IF chains (Figure 1, green). Furthermore, some sets, which occupy *e* and/or adjacent *g* heptad positions, have been precisely conserved (red). These are Glu-22 (*e*) in the 1A rod domain segment; Arg-12 (*e*), Glu-84 (*g*) and Lys-89 (*e*) in 1B; and Glu-106 (*g*) and Arg-111 (*e*) in 2B.

First, we made conservative changes by substituting the conserved Glu residues to Asp residues. The most dramatic effect on IF formation occurred for residue Glu-106 in 2B: substitution in one chain to Asp resulted in very short IF (Figure 2e) (Yang *et al.*, 1999); substitutions to Asp in both chains resulted in mostly unit-length particles (Figure 2f). In contrast, for the Glu-22 (in 1A) and Glu-84 (in 1B) positions, normal but somewhat shorter 2- to 5-μm-long IF formed (data are summarized in Table 3). However, when we substituted the Glu residue in one chain to an Ala residue, mostly subfilamentous particles 50–75 nm long were formed for the Glu-106 position (Figure 2g), whereas for the 1A Glu22Ala (Figure 2b) and 1B Glu84Ala (Figure 2c) substitutions, notably shorter IF, but still of normal morphology, were formed. Second, we performed cell transfection experiments with the use of K14-GFP plasmid constructs. Compared with wild-type K14 (Figure 3A), the Glu106Asp mutation resulted in a severely disrupted cytoskeleton (Figure 3K), but the similar Glu22Asp in 1A (Figure 3B) or Glu84Asp in 1B had little or no apparent effect (Table 3). In a series of Glu-to-Ala substitutions, we found again that the Glu106Ala mutation resulted in near total collapse of the IF network onto a perinuclear region and major deposits of spots of K14-GFP mutant protein toward the cell periphery (Figure 3L). These spots presumably contain accumulations of K14-GFP chains that cannot participate in the normal dynamic cytoskeletal organization. In contrast, the Glu22Ala in 1A (Figure 3C) and Glu84Ala in 1B (Figure 3F) resulted in near-normal IF cytoskeletons, although there was some evidence for elongated aggregates of IF bundles. Third, we made a series of substitutions in charged residue positions that have not been conserved in the IF chain family. In the following cases, none resulted in severe changes in keratin IF formed in vitro or cytoskeletons in vivo: Lys1Met and Lys17Met in 1A; Arg12Met, Asp56Glu or Asp56Ala (Figure 3B), and Lys89Met in 1B; and Lys4Met, Asp18Glu or Asp18Ala, Glu25Ala (Figure 3I) or Glu25Lys, Glu39Asp, Glu39Lys, or Glu39Ala (Figure 3J), and or Glu76Ala (Figure 2) in 2B. Fourth, we made a series of control mutants involving changes in other residue positions, including Arg19Leu in 1A and Glu54Ala and Lys71Ile in 1B. In no case did any of these notably affect IF assembly. Finally, we made what were thought to be a series of negative control substitutions. The Arg10Leu substitution in 1A resulted in total loss of IF, as expected (Fuchs and Weber, 1994; Irvine and McLean, 1999). The Arg111Leu substitution in the 2B rod domain segment resulted in only subfilamentous or unit-length IF particles in vitro and severely disrupted cytoskeletons in vivo (Table 3), as expected, because this residue position is thought to be an integral part of the molecular overlap/helix

Table 3. Affects of mutant chains on keratin IF assembly in vitro and in vivo

	In vitro assembly					In vivo assembly		
	K5	K14	Figure	Description		K14-GFP	Figure	Description
	Wild type	Wild type	2a	Normal	>10 μm	Wild type	3A	Normal
1A	Lys17Met	Wild type		Shorter	>2 μm			
	Glu22Asp	Wild type		Normal	≈10 μm	Glu22Asp	3B	Normal
	Glu22Asp	Glu22Asp		Normal	≈5 μm			
	Glu22Ala	Wild type	2b	Short	≈1 μm	Glu22Ala	3C	Abnormal
	Wild type	Glu22Ala		Short	≈1 μm			
1B	Wild type	Asp56Glu		Normal	>10 μm	Asp56Glu		Normal
	Wild type	Asp56Ala		Normal	>5 μm	Asp56Ala	3D	Normal
	Wild type	Glu75Ala		Normal	>5 μm			
	Wild type	Lys82Glu		Normal	>2 μm			
	Glu84Asp	Wild type		Normal	>5 μm			
	Glu84Asp	Glu84Asp		Shorter	>2 μm	Glu84Asp	3E	Normal
	Glu84Ala	Wild type	2c	Short	≈1 μm	Glu84Ala	3F	Abnormal
	Wild type	Glu84Lys		Shorter	≈2 μm	Glu84Lys	3G	Normal
	Lys89Met	Wild type		Shorter	>2 μm			
2B	Asp18Glu	Wild type		Normal	>10 μm			
	Asp18Ala	Wild type		Wider	>10 μm			
	Lys23Ile	Wild type		None				
	Wild type	Lys23Ile		None		Lys23Ile	3H	Disrupted, spots
	Glu25Ala	Wild type		Normal	>5 μm	Glu25Ala	3I	Normal
	Glu25Lys	Wild type		Normal	≈5 μm			
	Wild type	Glu39Asp		Normal	>10 μm			
	Wild type	Glu39Ala		Shorter	>2 μm	Glu39Ala	3J	Normal
	Wild type	Glu39Lys		Shorter	>2 μm			
	Lys44Glu	Wild type		Normal	5 μm			
	Wild type	Glu76Ala	2d	Shorter	>2 μm			
	Wild type	Glu104Asp		Normal	>5 μm			
	Asp104Glu	Wild type		Normal	≈10 μm			
	Asp104Glu	Glu104Asp		Normal	>5 μm			
	Wild type	Glu104Ala		None				
	Asp104Lys	Wild type		None				
	Glu106Asp	Wild type	2e	Very short	<1 μm			
	Wild type	Glu106Asp		Very short	<1 μm	Glu106Asp	3K	Disrupted, spots
	Glu106Asp	Glu106Asp	2f	None				
	Glu106Ala	Wild type	2g	None				
	Wild type	Glu106Ala		None		Glu106Ala	3L	Disrupted, spots
	Wild type	Glu106Lys		None		Glu106Lys		Disrupted, spots
	Wild type	Arg111Leu		None		Arg111Leu		Disrupted, spots
	Arg111Asp	Wild type	2h	Short	≈1 μm			

termination motif (Steinert *et al.*, 1993a,b,c). However, the Arg111Asp mutant formed less stable molecules and tetramers but formed short IF (Figure 2h).

Together, these results show that changes of most charged residue positions singly have only limited effects on IF structure in vitro or in vivo. Changes of the conserved residue positions Lys-1 or Glu-22 in 1A, Arg-12 or Glu-84 in 1B, and Lys-4 in 2B allowed the formation of IF of normal morphology, although of modestly reduced length, and modest (or no) changes in IF cytoskeletons. However, changes in the conserved Glu-106 residue of the 2B domain resulted in loss of IF.

Cross-Linking Studies with DST in Urea Solutions to Assess Dimer and Tetramer Stabilities Reveal Multiple Interactions

Previously, we established a simple method to assess the stabilities of single coiled-coil molecules and small assemblies of them with the use of a urea titration assay followed by cross-linking with the bifunctional reagent DST. This method was used here in an attempt to establish the molecular basis of the apparent critical importance of the residue positions identified above. At a concentration of ≈40 μg/ml in standard assembly buffer in the absence of urea, wild-type K5 and K14 chains form mostly tetramers, consisting of a pair of heterodimer molecules, as well as minor amounts of one-, three-, and four-molecule assemblies (Steinert *et al.*, 1993a). These tetramers dissociate into single molecules at ~6 M, and then the molecules dissociate into individual chains with ~9 M urea, as expected from the observations of Wawersik *et al.* (1997) and as suggested by our work with vimentin and α-internexin molecules (Steinert *et al.*, 1999) (Figure 4; all data are summarized in Table 4). Based on these IF assembly experiments, initially we examined several substitution constructs involving changes in charge in either K5 or K14,

Table 4. Summary of molecular stabilities of mostly single mutant chain mixtures in concentrated urea solutions

	Composition		Urea concentration (M) of half disassembly		
	K5	K14	Tetramer	Dimer	Figure
	Wild type	Wild type	6	9	4A
1A	Wild type	Lys01Met	5.5	>8	
	Lys17Met	Wild type	6	8	
	Wild type	Arg19Leu	5.5	7.5	
	Glu22Asp	Wild type	5.5	9	
	Glu22Asp	Glu22Asp	5	8.5	
	Glu22Ala	Wild type	5	7	4B
1B	Wild type	Arg12Met	6	8	
	Glu54Ala	Wild type	6	8.5	
	Wild type	Asp56Glu	6	9	
	Wild type	Asp56Ala	5.5	8.5	4C
	Wild type	Glu75Ala	5	8	
	Wild type	Glu79Ala	5	8	
	Asp79Ala	Wild type	5.5	8	
	Wild type	Lys82Glu	5	8	
	Lys71Ile	Wild type	3.5	8.5	
	Glu84Asp	Wild type	5.5	9	
	Glu84Asp	Glu84Asp	5.5	8.5	
	Glu84Ala	Wild type	5	6	
	Lys89Met	Wild type	5.5	7.5	
2B	Wild type	Lys04Met	6	>8	
	Asp18Glu	Wild type	6	9	
	Asp18Ala	Wild type	6	8.5	
	Arg20Leu	Wild type	5.5	8.5	
	Wild type	Lys23Ile	<1	8.5	4D
	Lys23Ile	Wild type	<1	8.5	
	Glu25Ala	Wild type	6	8.5	4E
	Wild type	Glu39Asp	6	9	
	Wild type	Glu39Ala	6	8.5	
	Wild type	Glu76Ala	6	8.5	
	Lys100Met	Wild type	<1	1	
	Asp104Glu	Glu104Asp	5.5	8.5	
	Asp104Ala	Wild type	<1	1	
	Asp104Lys	Wild type	<1	1	
	Wild type	Glu106Asp	3	9	4F
	Glu106Asp	Wild type	3	9	
	Glu106Asp	Glu106Asp	1	8.5	4G
	Glu106Ala	Wild type	<1	2	4H
	Wild type	Glu106Lys	<1	8.5	4I
	Wild type	Thr109Lys	5	8	
	Wild type	Thr109Asp	5	8	
	Wild type	Thr109Phe	1	3	
	Arg111Leu	Wild type	<1	1	4J
	Arg111Asp	Wild type	5	8.5	

and four principal observations became apparent. First, some substitutions (single-chain changes of 2B Lys23Ile and Glu106Lys, a double-chain change of 2B Glu106Asp) (Figure 4; Table 4) caused major losses in the stability of the tetramers but little apparent change in the stabilities of the single heterodimer molecules. Second, some substitutions involving changes of charge (2B Lys100Met, Asp104Ala, Asp104Lys, Glu106Ala, and Arg111Leu) destabilized both tetramers and single molecules, whereas Arg111Asp caused little change in stability. Third, mutations in a single chain in the conserved 1A Lys-1 or Glu-22 and 1B Arg-12 or Glu-84 positions caused only minor reductions in stability of the tetramers and single molecules. Fourth, a variety of other charge changes in other residue positions caused few detectable changes in stabilities.

Together, these data reveal that there are at least two separate types of interactions involving the conserved position Glu-106 in the 2B rod domain segment: one involves the stability of the heterodimer molecule, and thus might identify a potential trigger motif required for the coiled-coil molecules; and a second potentially involves stabilization of

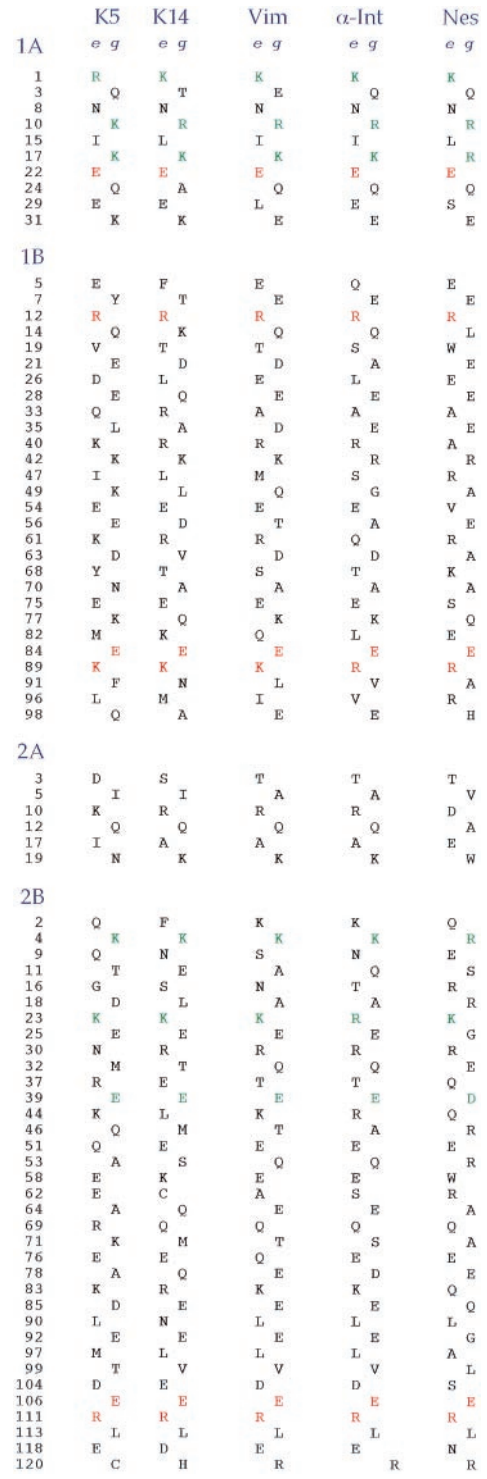

Figure 1. Presence of conserved sets of charged residues in IF chains. Some positions are conserved in charge across the entire family of IF chains (green), but a few others, restricted to the *e* and *g* heptad positions, have been precisely conserved (red), including lamins. Vim, vimentin; α-Int, α-internexin; Nes, nestin.

the two-molecule (and/or higher) stage of assembly. Accordingly, additional experiments were performed to test these two concepts separately.

Identification of Four Key Residue Positions in the Conserved 2B Region That Support the Presence of a Stabilizing Coiled-Coil Trigger Motif

As shown in Table 1, 7 of the 13 residue positions of the consensus trigger motif have specific residue-type requirements within the context of the regular *a-g* heptad repeat. Of potential motifs in the 1A, 1B, and 2B rod domain segments, that in the 2B region affords a good fit, having only an average of one or two variances from the proposed motif across the spectrum of mammalian IF chains. To further explore the role of the 2B region, we mutated four residue positions to examine their effects on molecular stabilities. First, the consensus trigger motif requires that the fourth residue position (residue position 104 of 2B) should be a Glu residue. We have noted that position 104 is indeed always acidic in IF chains, but often an Asp, whereas in the case of vimentin, it is now proposed to be in position to form an intrachain ionic salt bond with the similarly conserved Lys-100 residue (Herrmann *et al.*, 2000). When Asp104Glu (K5) and Glu104Asp (K14) were mutated and assembled either singly with the wild-type partner or together, we noted no ill effects on IF assembly in vitro (Table 3). Likewise, the one- and two-molecule assemblies with the doubly mutated chains were about as stable as the wild-type controls (Table 4). However, instead, when this position was discharged to an Ala or changed to a Lys residue in only one chain, no IF formed (Table 3), and the molecules were unstable even in 1 M urea (Table 4). We also mutated the conserved Lys-100 residue to Met and documented a marked loss of dimer stability (Table 4). These data suggest that position 4 should be acidic, either a Glu or an Asp. Second, position 6 (residue position 106 of 2B) should be charged. The foregoing data have established that this must be a Glu residue to form IF. However, mutants in one or both chains in which this is changed to an Asp or Lys (retention of a charge) form molecules that are about as stable as wild type, but Ala mutants (loss of charge) do not form stable molecules (Table 4). These data are in accordance with the proposed trigger motif. Third, position 9 (residue position 109 in 2B) should be charged, but in many IF chains, it is a Thr residue instead. We found that the Lys and Asp (charged) mutants formed molecules and tetramers of near normal stabilities (Table 4) and formed short IF in vitro (Table 3). However, the Phe (not charged) mutant did not form IF (Table 3), and molecules and tetramers appeared by this assay to be rather less stable (Table 4). Thus, for IF a hydrophilic residue or a short-chained aliphatic residue at position 9 is acceptable. Finally, position 111 should be charged. Our data described above document that the Asp mutant forms short IF in vitro (Table 3; Figure 4J) and stable molecules (Table 4), but a loss-of-charge Leu mutant did not form IF or stable molecules (Table 4; Figure 4J). Together, these data are consistent with the possible existence of a trigger motif between residues 100 and 113 of the 2B rod domain segment that contributes importantly to molecular stability.

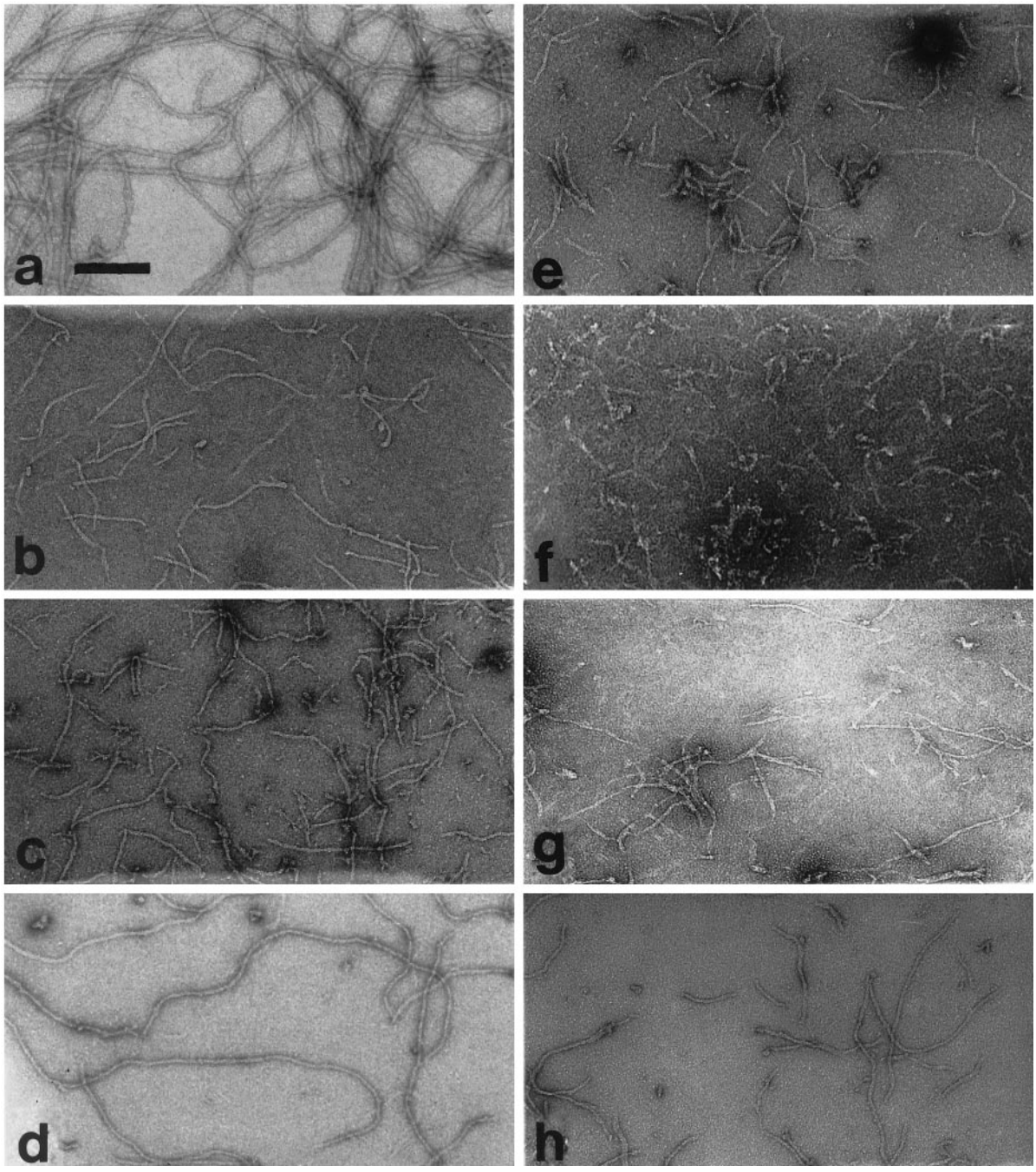

Figure 2. Electron microscopy of IF assembled from wild-type and/or mutant K5/K14 chains. These and all data are summarized in Table 3. (a) Wild type; (b) K5 1A Glu22Ala and K14 wild type; (c) K5 1B Glu84Ala and K14 wild type; (d) K5 wild type and K14 2B Glu76Ala; (e) K5 2B Glu106Asp and K14 wild type; (f) K5 2B Glu106Asp and K14 2B Glu106Asp; (g) K5 2B Glu106Ala and K14 wild type; (h) K5 2B Arg111Asp and K14 wild type. Bar, 200 nm.

Evidence for a Stabilizing Trigger Motif in the 1B Domain

As reported above, single-charge changes in the vicinity of the putative trigger motifs documented in Table 1 in either the K5 or K14 chain in the 1A and 1B segments had only limited effects on molecular stability and IF assembly. We repeated the urea stability experiments by coassembly of different mutant forms of both the K5 and K14 chains that involved multiple charge changes in the vicinity of the putative trigger motifs (all gel data are summa-

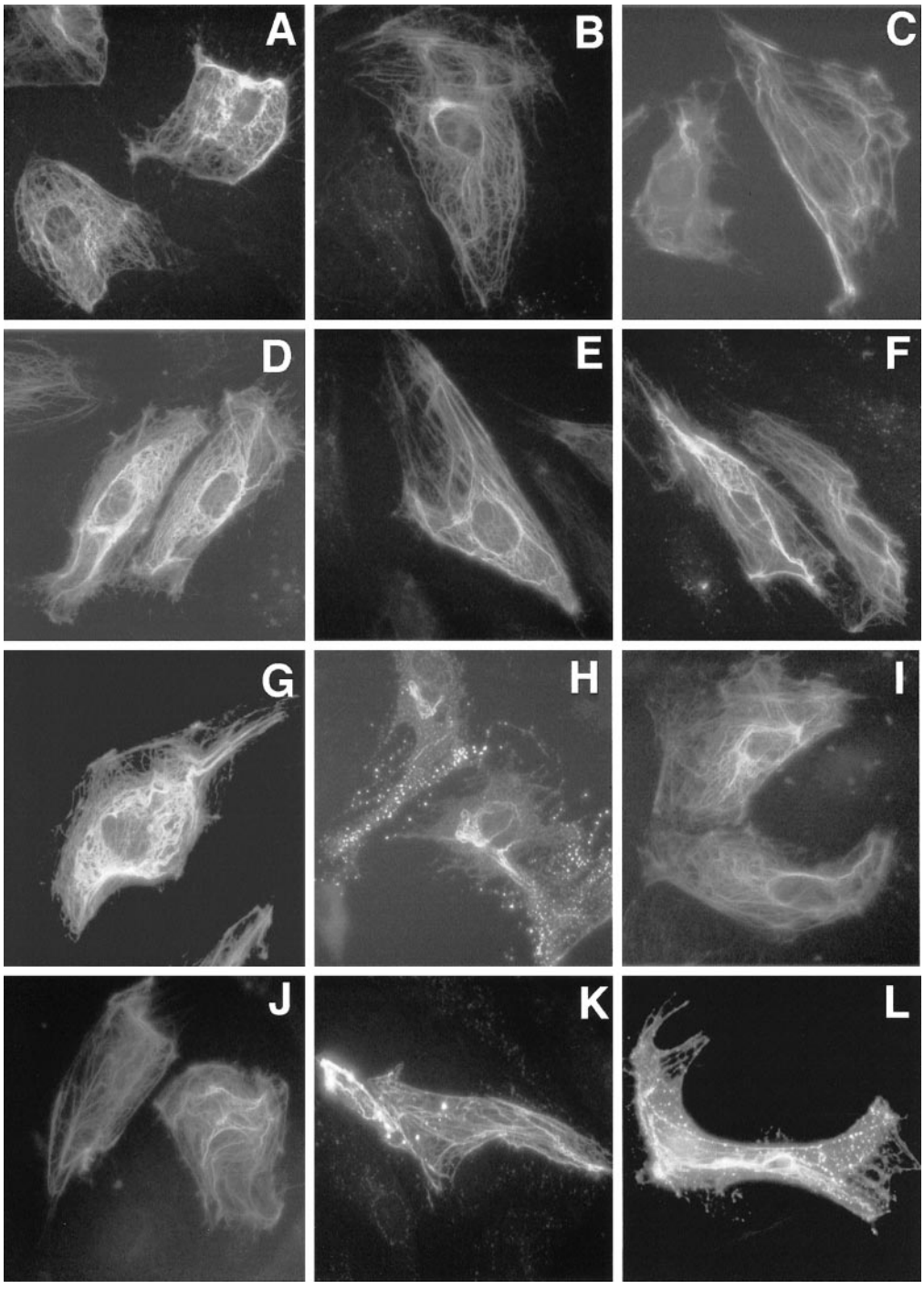

Figure 3. Direct immunofluorescence of wild-type and mutant K14-GFP constructs transfected into PtK2 cells. These and all other data are summarized in Table 3. (A) Wild type; (B) 1A Glu22Asp; (C) 1A Glu22Ala; (D) 1B Asp56Ala; (E) 1B Glu84Asp; (F) 1B Glu84Ala; (G) 1B Glu84Lys; (H) 2B Lys23Ile; (I) 2B Glu25Ala; (J) 2B Glu39Ala; (K) 2B Glu106Asp; (L) 2B Glu106Ala.

rized in Table 5). In the case of the 1A domain region, four pairs of double mutants involving the conserved residue Glu-22 and one of several neighboring charged residues still had only minor effects on molecular and tetramer stabilities. However, in 1B, major losses of stability occurred only for those double mutants that traversed the residue positions from ~75 to 89. In particular, loss by discharging of one of the conserved residues (Glu-84 or Lys-89), together with loss on one chain of another nearby

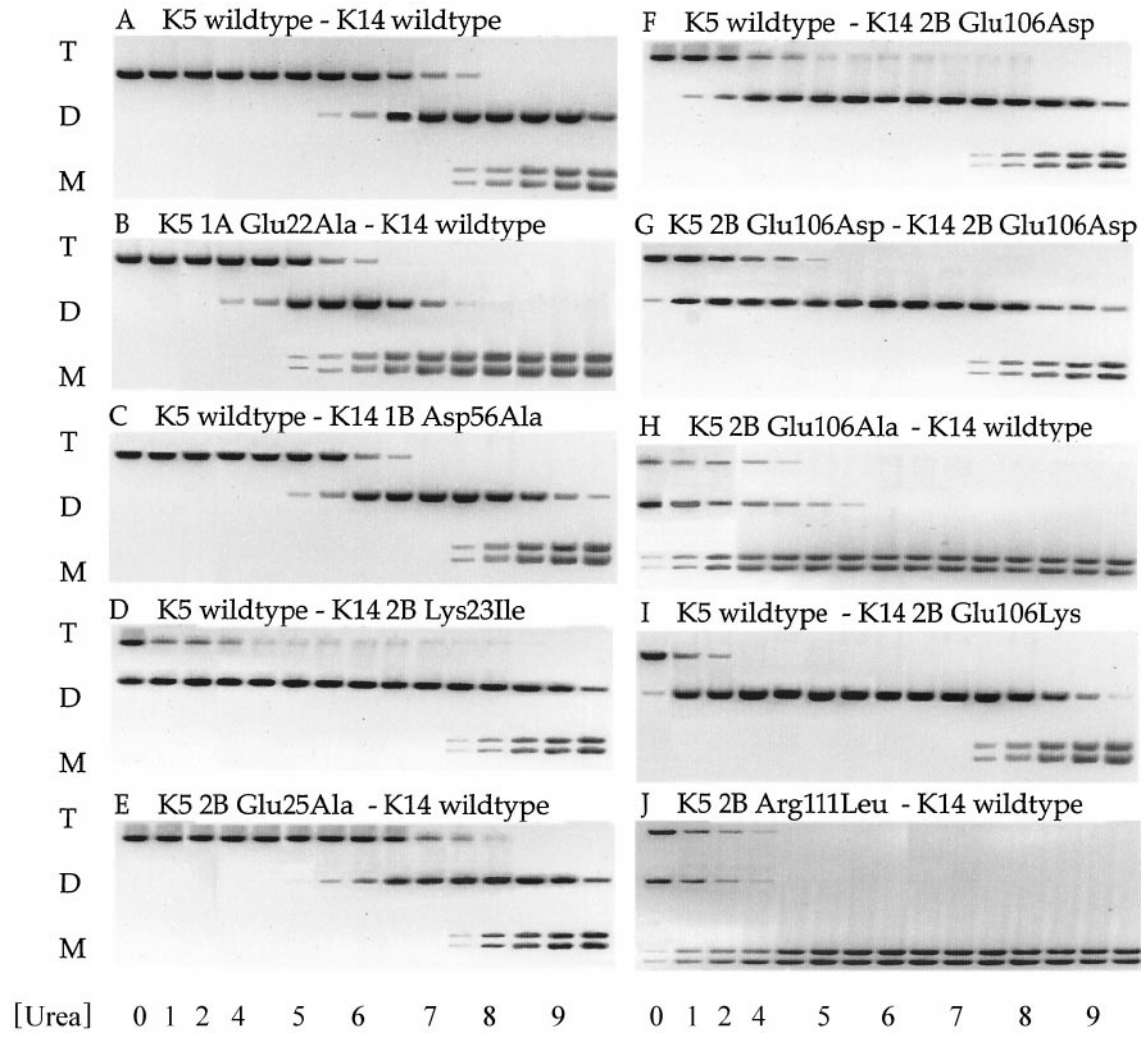

Figure 4. Stabilities of dimer (one-molecule) and tetramer (two-molecule) assemblies of wild-type and/or mutant chains in concentrated urea solutions (as shown) after cross-linking. These and all other data are summarized in Tables 4 and 5. (A) Wild type; (B) K5 1A Glu22Ala and K14 wild type; (C) K5 wild type and K14 1B Asp56Ala; (D) K5 wild type and K14 2B Lys23Ile; (E) K5 2B Glu25Ala and K14 wild type; (F) K5 wild type and K14 2B Glu106Asp; (G) K5 2B Glu106Asp and K14 2B Glu106Asp; (H) K5 2B Glu106Ala and K14 wild type; (I) K5 wild type and K14 2B Glu106Lys; (J) K5 2B Arg111Leu and K14 wild type. T, D, and M mark the positions of migration of the tetramer, dimer, and monomer species, respectively.

charged residue, promoted destabilization of the molecules. In addition, loss of two charged residues in the vicinity of and with maintenance of the conserved charged residues in the 1B region also destabilized the molecules. Thus, these data support the possibility of the existence of a stabilizing trigger-like motif in the 1B domain but not in the 1A domain.

Lys-23 of the 2B Rod Domain Segment Is Absolutely Required for Normal IF Assembly In Vitro and In Vivo

In addition, we have noted that position 23 of the 2B rod domain segment is usually basic (including type V lamins). We found that the Lys23Ile substitution of this position resulted in completely failed IF assembled in vitro, in which only subfilamentous particles formed (Table 3), and in vivo (Figure 3H), in which most of the keratin IF cytoskeleton had collapsed and the K14-GFP mutant protein had accumulated in spots. Indeed, the phenotype in both cases was similar to charge changes of position Glu-106. Furthermore, like Glu-106, this substitution allowed the formation of stable molecules, but tetramers formed from it were unstable (Figure 4D). However, the nearby substitutions Asp18Ala and Arg20Leu of the K5 chain had little affect on molecular or tetramer stabilities (Table 4).

The Glu-106 and Lys-23 Residues of the 2B Rod Domain Segment Are Required for the Stability of the A_{22} Mode of Alignment of Two Molecules

The data shown in Figure 4 and Table 4 confirm the long-established concept that subcritical concentrations of wild-

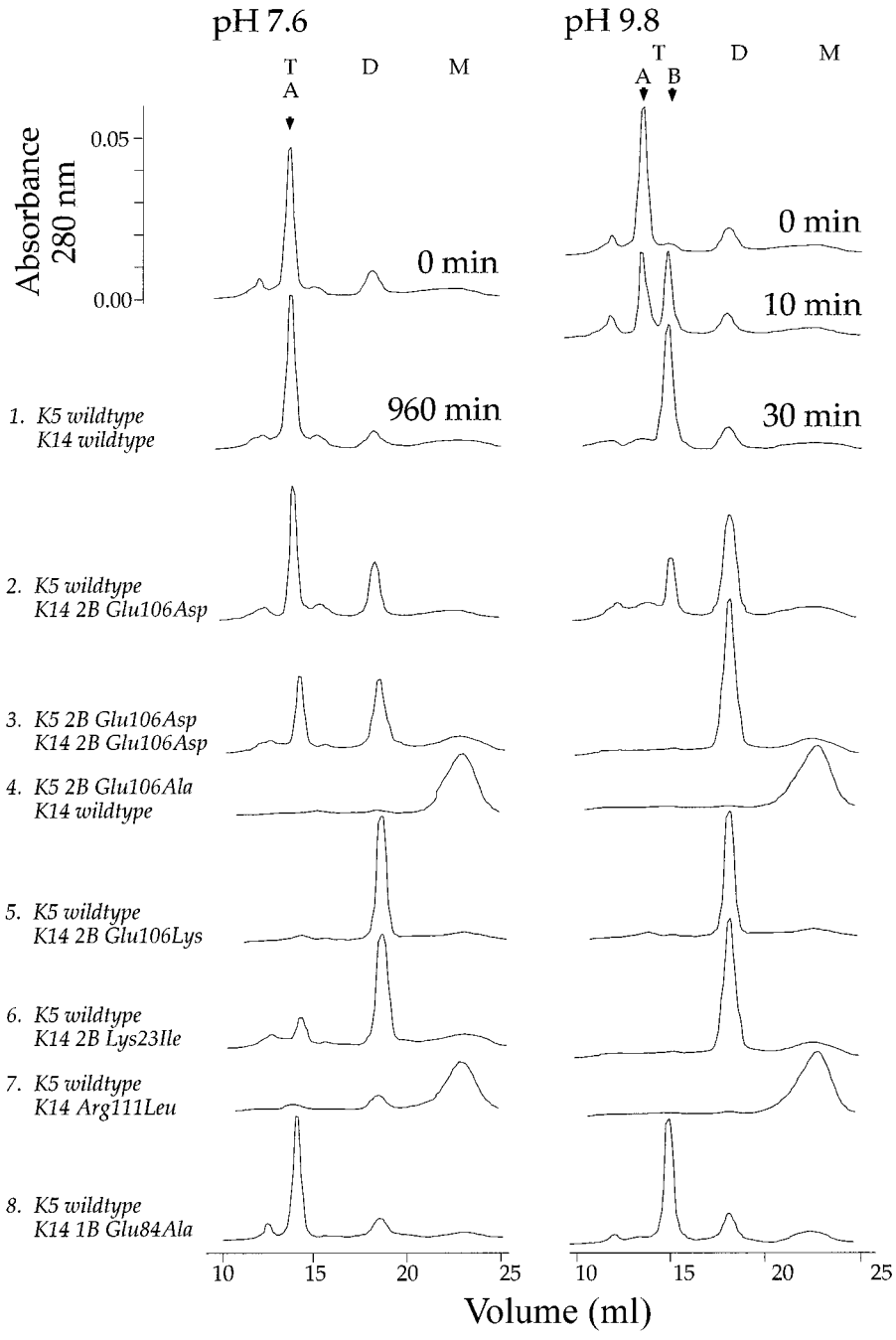

Figure 5. Chromatography on Sepharose CL400 of particles formed below the critical concentration of assembly and at pH values of 7.6 (left column) and pH 9.8 (right column). For wild-type IF at pH 7.6, most of the particles consist of tetramers (A), but at pH 9.8, most of the particles move to an alternatively sized tetramer (B) within ≤30 min. Seven other wild-type and/or mutant IF assemblies were then examined as shown. T, D, and M mark the positions of elution of the tetramer, dimer, and monomer species, respectively.

type keratins (and many other IF types) in optimal IF assembly buffers form primarily tetramers, i.e., pairs of molecules. Indeed, when chromatographed on a Sepharose column, a single peak was observed (Figure 5), which, when examined after negative staining, was seen to consist largely of particles that were 60–70 nm long (Figure 6, A and C). These dimensions are expected for the alignment of two molecules in the A_{11} and/or A_{22} mode (Steinert, 1991). In the cases of the single and double Glu106Asp mutants, the amounts of this tetramer peak were reduced by ~25 and 50%, respectively, and were fully lost with the Glu106Ala and Lys23Ile mutants. This loss of the tetramer peak indicates the loss of stability of either the A_{11} or A_{22} mode of alignment, leading to the loss of both. In these cases, as seen in Figure 4, a dimer peak appeared that could not be adequately visualized by the methods used for electron microscopy but that presumably consisted of a single molecule ~46 nm in length. In three additional control experiments with mutant chains, all of the protein was recovered as the single molecule species or appeared as a monomer protein, as expected from the foregoing molecular stability data. Molecules

Table 5. Summary of molecular stabilities of double-mutant chain mixtures in concentrated urea solutions

	Composition		Urea concentration (M) of half disassembly	
	K5	K14	Tetramer	Dimer
1A	Lys17Met	Lys17Met	5.5	7.5
	Lys17Met	Arg19Leu	4	5
	Glu22Ala	Arg19Leu	4.5	5.5
	Glu22Ala	Glu22Ala	4	6
1B	Glu54Ala	Asp56Ala	5	8
	Glu54Ala	Glu75Ala	4.5	7
	Glu54Ala	Glu79Ala	4.5	6
	Glu54Ala	Lys82Glu	5	7
	Lys71Ile	Glu75Ala	4.5	7
	Lys71Ile	Lys82Glu	4.5	6.5
	Lys71Ile	Glu84Lys	4	6
	Asp79Ala	Glu75Ala	4	6
	Asp79Ala	Lys82Glu	<1	<1
	Asp79Ala	Glu84Lys	<1	<1
	Glu84Ala	Asp56Ala	4.5	6
	Glu84Ala	Glu75Ala	1	2
	Glu84Ala	Glu79Ala	<1	<1
	Glu84Ala	Lys82Glu	<1	<1
	Lys89Met	Asp56Ala	4	6.5
	Lys89Met	Glu75Ala	<1	<1
	Lys89Met	Glu79Ala	<1	<1
	Lys89Met	Lys82Glu	<1	<1
2B	Asp18Ala	Glu39Ala	6	8.5
	Asp18Ala	Glu76Ala	5	8
	Asp18Ala	Glu106Asp	2	3
	Glu25Ala	Glu39Ala	5.5	8
	Glu25Ala	Glu76Ala	5.5	8
	Glu25Ala	Glu106Asp	2	3
	Glu25Ala	Thr109Lys	1	3
	Arg111Asp	Glu106Asp	2	4
	Arg111Asp	Thr109Lys	<1	<1

formed with the 1B Glu84Ala mutant formed tetramers with wild-type properties, as expected.

When the keratin IF proteins were equilibrated in solution at pH 9.8 instead, the tetramer peak shifted to a slightly smaller apparent molecular size within 30 min (shift from peak A to peak B in Figure 5). The peak B tetramers were 45 nm long (Figure 6, B and D) and are thus consistent with the alignment of two molecules in the A_{12} mode (Aebi *et al.*, 1988; Steinert, 1991). In this case, chromatography of the single and double Glu106Asp mutants resulted in only a minor amount of the A_{12} tetramer, or none at all, as protein was chased into the single molecule peak.

These data suggest that the conserved Lys-23 and Glu-106 positions of the 2B rod domain are required for stabilization of the two-molecule stage of IF assembly. As a further test, we cross-linked mixtures of wild-type and mutant chains at subcritical protein concentrations (≈40 μg/ml) with DST after dialyzing into assembly buffer for 1–8 h. We show that for the Glu106Asp, Glu106Lys, and Lys23Ile mutants, all tetramer species were lost in 2–6 h (Figure 7). To examine which mode of alignment might be of critical importance, we performed larger-scale cross-linking reactions on mixtures that had been equilibrated for ≤2 h. The proteins were then cleaved with cyanogen bromide and digested with trypsin, and the peaks were recovered by HPLC as described previously (Steinert *et al.*, 1993b). In the case of wild-type K5/K14 oligomers, 15 shifted peaks were shown by limited sequence analyses to contain peptides cross-linked through the same juxtaposed Lys residues and in similar yields, as identified previously. Each of these could be unambiguously assigned to either the A_{11} or A_{22} mode of alignment of two molecules. Semiquantitative data were assessed based on the areas of the peaks (Table 6). We found that there were ~1.36 mol of cross-links/mol of heterodimer in the A_{11} alignment and ~0.45 mol/mol in the A_{22} alignment. These values presumably reflect the presence of fewer optimally placed Lys residues defining the A_{22} mode. These experiments were repeated for six other mixtures of wild-type and/or mutant chains. Notably, in the cases of the 2B Glu106Asp single and double mutants and the 2B Lys23Ile mutant, the yields of the cross-links that define the A_{22} alignment were greatly reduced or completely lost, whereas those that define the A_{11} alignment were retained, although they were reduced by 30–50% after a 2-h equilibration. Similarly, in the case of the Glu106Ala mutant, in which <25% of the protein remains as tetramers after 2 h in assembly buffer (Table 3; Figures 3 and 7), most of the cross-links defining the A_{11} mode were retained, but none were found for the A_{22} mode. In the cases of the 1A Glu22Ala and 1B Glu84Ala mutants, all cross-links that define both the A_{11}

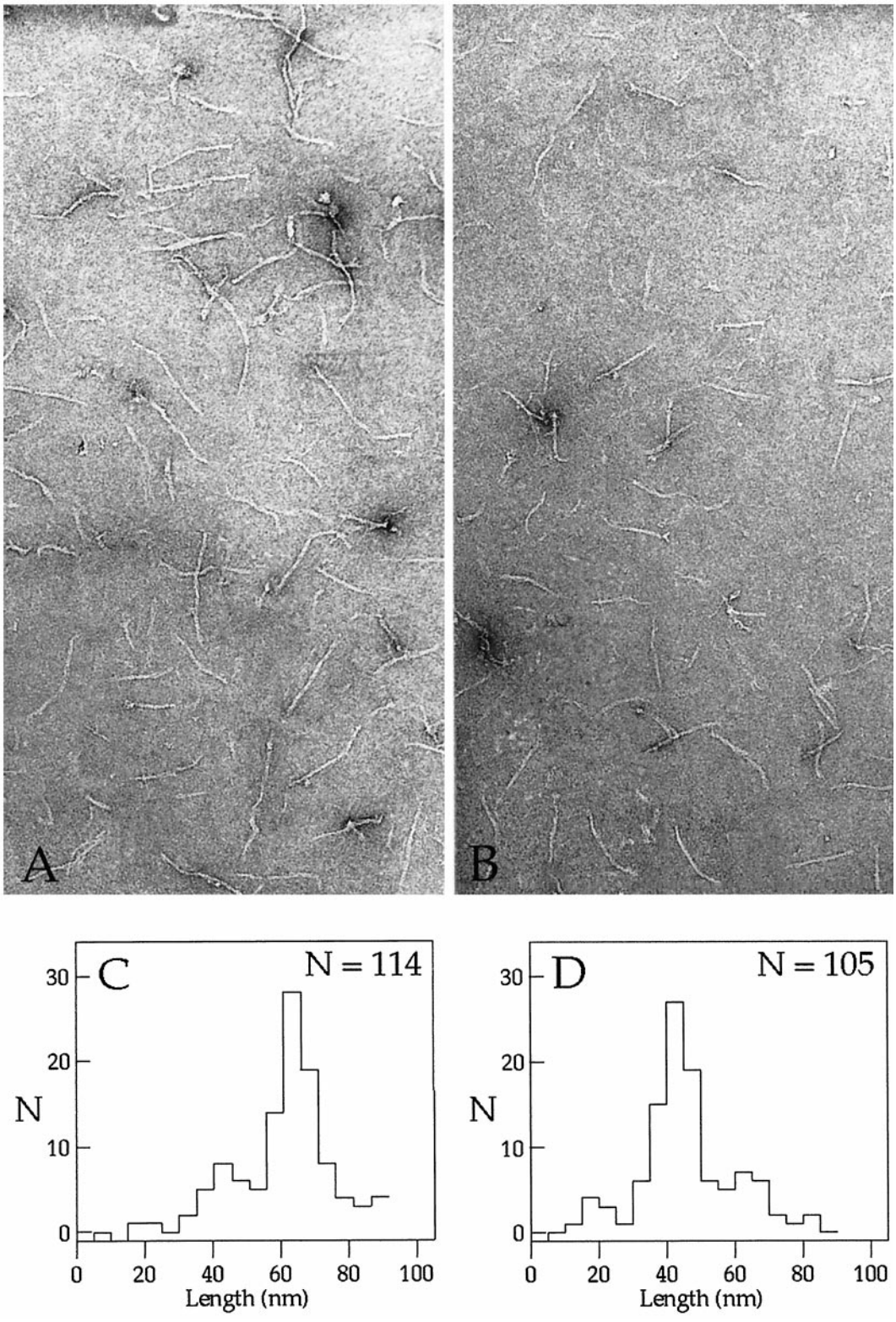

Figure 6. Electron microscopy of tetramer peaks recovered from the Sepharose CL400 column. (A) Peak A from a column run at pH 7.6; (B) peak B from a column run at pH 9.8. These particles are tetramers and are ~65 nm (C) or 45 nm (D) long. Particles were visualised by negative staining with 0.3% uranyl acetate over a carbon-coated holey film grid.

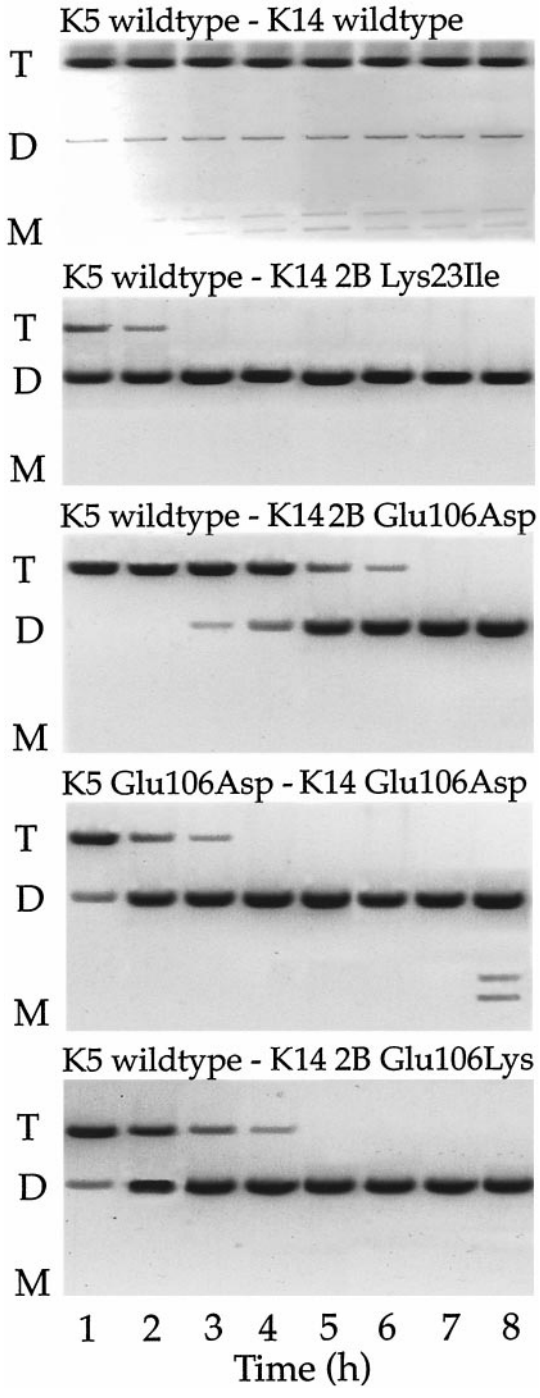

Figure 7. Stabilities of tetramers in assembly buffer solution. Mixtures of wild-type and/or mutant chains in concentrated urea solutions were equilibrated into assembly buffer for the times shown and then cross-linked with DST. T, D, and M mark the positions of elution of the tetramer, dimer, and monomer species, respectively.

and A_{22} alignments were retained, with yields that were reduced by only 20% or less. Accordingly, these data reaffirm our earlier conclusions that the A_{11} and A_{22} alignment modes of the tetramer coexist in solution. Furthermore, mutation of Lys-23 or Glu-106 of the 2B rod domain segment causes destabilization of the A_{22} mode, leading to loss of all tetramers. These data suggest that the A_{11} and A_{22} modes of alignment exist in solution in an equilibrium mixture that apparently favors A_{22}; loss of it by destabilization thus results in the slow loss over several hours of all tetramers (Figure 7).

DISCUSSION

Evidence That IF Chains Possess a Coiled-Coil Trigger Sequence Motif toward the End of Their 2B Rod Domain Segments

Recent analyses of a variety of proteins known to form long two-chain coiled coils have revealed the presence of a 13-residue motif, often but not always sited toward the ends of the heptad sequence region, that affords special stability to coiled-coil formation (Kammerer *et al.*, 1998; Steinmetz *et al.*, 1998; Burkhard *et al.*, 2000). This trigger is thought to stabilize the coiled coil by a network of favorably oriented residues of certain types within the *a-g* heptad background. However, it remains to be determined whether the island of stability at the trigger fosters the initiation of coiling or is otherwise involved in coiled-coil assembly.

In this paper, we have addressed the question of whether such motifs also exist in IF chains and are important for IF structure. However, the exact motif as currently defined is not present in IF chains, but the best matches occur toward the ends of the 1A, 1B (two overlapping locations), and 2B rod domain segments (Table 1). The region showing the fewest number of consensus mismatches is in the 2B segment, partly overlapping the "helix termination" motif. The most common mismatches occur at residue positions 4 (predicted to be a Glu residue, but more commonly an Asp in IF proteins) and 9 (which is most often a hydrophilic Thr instead of a predicted charged residue). Nevertheless, several mutations at positions 4 (Glu-104), 6 (Glu-106), 9 (Thr-109), or 11 (Arg-111) generated in this study result in notably or completely destabilized molecules. Conversely, these are consistent with the notion that this region affords special stability to coiled coils and thus may function as a trigger motif. This evidence comes from our analysis of the stabilities of dimer molecules in concentrated urea solutions. Thus, mutations of Glu-106 to Asp or Lys or Arg-111 to Asp in either the K5 or K14 chain, or both, formed dimer molecules that were stable at urea concentrations >6 M (Table 4), although most could no longer form IF. Moreover, mutations that removed the charge (Asp104Ala, Glu106Ala, and Arg111Leu) failed to form stable dimer molecules. This loss of dimer stability cannot be attributed simply to loss or change of a single charge on the entire molecule because point charge substitutions at 18 other sites along the K5 or K14 chains allowed the formation of dimers stable at >6 M urea (Table 4). In the case of position 4, our mutational data indicate that either a Glu or an Asp afford comparable stabilities in the case of keratin IF molecules. For position 9, our data and the wild-type protein data indicate that several types of residues possessing short side chains may be used successfully in this position in IF, although a bulky side chain such as a Phe residue resulted in significant impairment (Table 4).

Table 6. Yields of peptides in the A_{11} and A_{22} two-molecule alignments (mol/mol)

Cross-link	K5: wt K14: wt	1A Glu22Ala wt	wt 1B Glu84Ala	wt 2B Glu106Asp	2B Glu106Asp 2B Glu106Asp	2B Glu106Ala wt	wt 2B Lys23Ile
A_{11} cross-links							
K5: 1A 10							
K14: 2A 19	0.07	0.05	0.10	0.05	0.07	0.02	0.09
K5: 1B 49							
K5: 1B 49	0.23	0.20	0.18	0.25	0.11	0.06	0.13
K5: 1B 40							
K5: 1B 61	0.06	0.02	0.05	0.03	0.03	0.01	0.02
K14: 1B 06							
K14: 1B 89	0.33	0.30	0.25	0.35	0.21	0.08	0.18
K5: 1B 06							
K5: 1B 42	0.11	0.09	0.07	0.09	0.05	0.03	0.03
K5: 1B 61							
K14: 1B 42	0.08	0.07	0.06	0.05	0.07	0.01	0.03
K5: 1B 89							
K14: 1B 06	0.03	0.02	0.02	0.01	0.00	0.00	0.00
K14: 1B 06							
K14: 1B 90	0.19	0.22	0.18	0.22	0.14	0.05	0.16
K5: 1A 17							
K5: 2A 10	0.23	0.25	0.20	0.31	0.19	0.05	0.15
K14: 1B 14							
K14: 1B 82	0.03	0.02	0.01	0.02	0.00	0.01	0.01
A_{22} cross-links							
K5: 2B 44							
K5: 2B 83	0.10	0.09	0.08	0.02	0.00	0.00	0.00
K5: 2B 23							
K5: 2B 100	0.04	0.05	0.05	0.00	0.00	0.00	0.00
K5: 2B 44							
K5: 2B 81	0.11	0.07	0.09	0.01	0.00	0.00	0.00
K5: 2A 10							
K14: E2 25	0.08	0.12	0.10	0.00	0.00	0.00	0.00
K5: 2B 45							
K5: 2B 83	0.12	0.06	0.08	0.01	0.00	0.00	0.00

Thus, our new mutational data favor the possibility that the sequence region encompassing residues 100–113 toward the end of the 2B rod domain segment in IF chains is especially important for the stability of the two-chain coiled-coil molecule for keratin IF. Therefore, this region may serve as a trigger motif for keratin IF.

Furthermore, except for positions 1 and 2 (residues 101 and 102), there is almost perfect sequence conservation in this region in all IF chains (Table 1). Accordingly, it seems plausible that this region may function the same way in all IF. The minor degrees of deviation seen here for IF molecules from the trigger consensus motifs of other coiled-coil proteins reported by Kammerer *et al.* (1998) may reflect the special or relaxed stability requirements of IF.

Recently, the three-dimensional structure of the last 35 residues of the 2B rod domain segment of human vimentin, including the trigger motif identified here, was presented (Herrmann *et al.*, 2000). Among a number of interesting features, the structure revealed the potential formation of an interchain ionic salt bond of the $1e - 2g'$ type involving the residues Glu-106 and Arg-111 and an intrachain ionic salt bond of the $i,i + 4$ type between residues Lys-100 and Asp-104 on each chain. However, it should be pointed out that further detailed biophysical analyses are required to establish whether such bonds do in fact form and whether they contribute favorable stability to the coiled-coil structure. These charged residues of vimentin also occur in the K5 and K14 chains (Table 1). Interestingly, our urea stability assays showed that discharging of either Glu-106 to Ala or Arg-111 to Leu destabilized molecules (Table 4). Furthermore, substitutions of Lys-100 to Met and Asp-104 to Ala or Lys resulted in unstable molecules. Accordingly, further detailed thermodynamic and kinetic analyses seem appropriate.

The Presence of a Potential Trigger Coiled-Coil Motif in the 1B Rod Domain Segment

Of the four regions in IF chains homologous to the consensus trigger (Table 1), we note that the one in the 1A region is not highly conserved among IF chains (Table 1). Furthermore, it contains three to four mismatches, at least two of which would seem to be problematic, including an uncharged residue at position 6 and an Asn residue at position 7 instead of a hydrophobic residue for the *d* heptad repeat position. Nevertheless, to address the question, we tested a series of K5 and K14 double mutants designed to separately discharge the conserved potential interchain interaction and other nearby residues (Table 5). We found that those in the 1A domain resulted in mole-

cules that were only slightly less stable to urea dissolution than other nonconserved residue positions (6–6.5 M urea) and that the IF formed in vitro or in vivo were near normal. Thus, we were unable to find strongly destabilizing residues, so that based on these data, we conclude that the 1A domain may not harbor a stabilizing coiled-coil trigger motif.

However, in the case of the 1B domain, there are two potential overlapping regions each with two or three deviations from the consensus motif that seem less serious: position 4 is typically not acidic in IF chains, and position 9 is usually aliphatic in IF chains instead of charged; furthermore, K5 has a mismatch at position 12. Based on the structural data for the 2B domain (Herrmann *et al.*, 2000), a large aliphatic residue at position 9 would fit, assuming the chain does not fold backward, as at the end of the 2B domain. Additionally, our data with double mutants revealed (Table 5) that loss of multiple charged residues in the vicinity of positions 75–89, and not elsewhere along the 1B segment, resulted in loss of molecular stability. These data thereby define residues 79–91 as a second potential stabilizing trigger (Table 1).

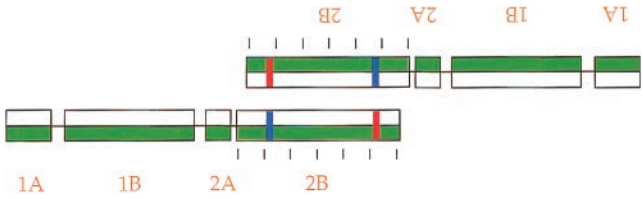

Figure 8. A model of two heterodimer keratin molecules (the two-chain types are shown in white and green) aligned in the A_{22} mode with the use of the statistically averaged displacement values determined from earlier cross-linking studies (Parry and Steinert, 1999). This model displays the close proximity of the two conserved 2B Glu-106 residues of one molecule (red lines) with the two conserved 2B Lys-23 residues (blue lines) of the other molecule. We propose that these may interact to contribute essential stability to the A_{22} alignment mode. Because the 2B Glu106Asp mutants do not assemble into normal IF, we speculate that the side chain of an Asp residue is not long enough to form these stabilizing interactions. This may afford a molecular explanation of one case of epidermolytic hyperkeratosis observed for the Glu106Asp substitution in the K1 chain (Yang *et al.*, 1999). The segments of the molecules are marked. A 20-residue scale is shown next to the 2B segments.

Why Are There at Least Two Potential Stabilizing Trigger Motifs in IF Chains?

In IF chains, the L12 region separates the long 1B segment (101 residues) from the long 2A + L2 + 2B segments (148 residues) (which remain α-helical or at least quasi-α-helical through L2 [North *et al.*, 1994]). L12 sequences, however, are unlikely to be α-helical and thus may involve a radical change in protein structure. Accordingly, we speculate that a total of at least two trigger motifs, one in 1B and another in 2B, may be required to stabilize and/or maintain the entire IF rod domain as a segmented coiled coil. Because our present data were unable to identify a functional trigger motif in the 1A domain, it is possible that the 1A domain may remain uncoiled. Indeed, very recent atomic resolution structural information by x-ray crystallography has documented that short constructs encompassing the 1A region only are not coiled (Strelkov *et al.*, 1999). Clearly, more biophysical and structural work will be necessary to confirm these ideas.

Evidence That the 2B Domain Glu-106 Residue Is Also Required for Stability of the A_{22} Mode of Molecular Assembly

A large body of chromatographic, ultracentrifugation, electron microscopic, solution birefringence, and cross-linking data have heretofore documented that tetramers of a variety of mammalian IF exist in solution as 60- to 70-nm-long particles in which the two molecules are associated in an antiparallel partially overlapped way in the A_{11} or A_{22} mode of alignment, or both. Our cross-linking data (Steinert *et al.*, 1993a,b,c, 1999) demonstrate that these two modes coexist in standard assembly buffer solutions, but they do not afford quantitative measurements of the amount of each. Although data have suggested that A_{11} is the favored mode in vimentin IF, perhaps because of the stability afforded by interactions of head and rod domain sequences (Herrmann and Aebi, 1998, 1999), our new data suggest that K5/K15 IF should be different. In cross-linking experiments, certain mutations (Glu106Asp or Glu106Lys and Lys23Ile of the 2B rod domain segment) resulted in loss of the A_{22} mode (Table 6), loss within 8 h of the A_{12} mode (Figure 5), and slow loss over a 2- to 6-h period of all tetramers (Figure 7). This could occur only if the A_{22} alignment mode is thermodynamically favored in solution. In other experiments not described here (our unpublished observations), we found evidence that the A_{22} mode is in fact significantly more stable than the A_{11} mode in the K5/K14 system in solution. Presumably, when the wild-type A_{22} mode is destabilized by mutation, it and the less stable wild-type A_{11} mode slowly dissociate to single molecules, a process that may occur by tetramer switching, as described previously (Aebi *et al.*, 1988; Steinert, 1991).

Therefore, why are the Glu-106 and Lys-23 positions so essential for the stability of the A_{22} mode? Despite the current absence of atomic resolution structural information, our earlier quantitative estimates of molecular alignments show that the two conserved Lys-23 residues on one molecule lie very close to at least one of the two conserved Glu-106 residues on a second molecule when a pair of molecules are aligned in the A_{22} mode (Figure 8) (Parry and Steinert, 1995, 1999). Thus, we speculate that these residues may interact and are critical for the stability of the A_{22} alignment mode. The nearby Asp-18 and Arg-20 residues of the K5 chain appear to be less essential (Table 4). Nevertheless, all of our new data indicate that the Glu-106 residue, which has been precisely conserved in all IF chains, appears to have dual roles in stabilizing both the first and second hierarchical levels of IF structure. Furthermore, we have been intrigued by the occurrence of a severe case of epidermolytic hyperkeratosis caused by an apparently conservative Glu106Asp mutation in one allele of the K1 chain (Yang *et al.*, 1999). This substitution affects IF assembly in vitro (Figure 2) and in vivo (Figure 3) and also tetramer stability (Figures 4 and

5) at the A_{22} molecular alignment mode (Table 6). Therefore, it is reasonable to speculate that the side chain of an Asp residue is simply not long enough to fulfill the key interactions required for stabilizing the A_{22} molecular alignment mode.

ACKNOWLEDGMENTS

We thank Dr. Robert Goldman for the kind gift of the K14-GFP construct and advice on the application of direct immunofluorescence methods. We thank Drs. Ueli Aebi, Harald Herrmann, and Alasdair Steven for valuable and stimulating discussions during the 2-year period of this work.

REFERENCES

Aebi, U., Haner, M., Troncoso, J., Eichner, R., and Engel, A. (1988). Structural features of intermediate filaments. Protoplasma *145*, 73–81.

Burkhard, P., Kammerer, R.A., Steinmetz, M.O., Bourenkov, G.P., and Aebi, U. (2000). The coiled-coil trigger site of the rod domain of cortexillin I unveils a distinct network of interhelical and intrahelical salt bridges. Struct. Fold. Des. *8*, 223–230.

Candi, E., Tarcsa, E., DiGiovanna, J.J., Compton, J.G., Elias, P.M., Marekov, L.N., and Steinert, P.M. (1998). A highly conserved lysine residue on the head domain of type II keratins is essential for the attachment of keratin intermediate filaments to the cornified cell envelope through isopeptide crosslinking by transglutaminases. Proc. Natl. Acad. Sci. USA *95*, 2067–2072.

Cohen, C., and Parry, D.A.D. (1990). Alpha-helical coiled coils and bundles: how to design an alpha-helical protein. Proteins *7*, 1–15.

Cohen, C., and Parry, D.A.D. (1994). Alpha-helical coiled coils: more facts and better predictions. Science *263*, 488–489.

Fuchs, E., and Weber, K. (1994). Intermediate filament structure, dynamics, function, and disease. Annu. Rev. Biochem. *63*, 345–382.

Harbury, P.B., Kim, P.S., and Alber, T. (1994). Crystal structure of an isoleucine-zipper trimer. Nature *371*, 80–83.

Heins, S., Wong, P.C., Müller, S., Goldie, K., Cleveland, D.W., and Aebi, U. (1993). The rod domain of NF-L determines neurofilament architecture, whereas the end domains specify filament assembly and network formation. J. Cell Biol. *123*, 1517–1533.

Herrmann, H., and Aebi, U. (1998). Intermediate filament assembly: fibrillogenesis is driven by decisive dimer-dimer interactions. Curr. Opin. Struct. Biol. *8*, 177–185.

Herrmann, H., and Aebi, U. (1999). Intermediate filament assembly: temperature sensitivity and polymorphism. Cell. Mol. Life Sci. *55*, 1416–1431.

Herrmann, H., Haner, M., Brettel, M., Ku, N.-O., and Aebi, U. (1999). Characterization of distinct early assembly units of different intermediate filament proteins. J. Mol. Biol. *286*, 1403–1420.

Herrmann, H., *et al.* (2000). The intermediate filament protein consensus motif of helix 2B: atomic structure and contribution to assembly. J. Mol. Biol. *298*, 817–832.

Irvine, A.D., and McLean, W.H.I. (1999). Human keratin diseases: the increasing spectrum of disease and subtlety of the phenotype-genotype correlation. Br. J. Dermatol. *140*, 815–828.

Kammerer, R.A., Schulthess, T., Landwehr, R., Lustig, A., Engel, J., Aebi, U., and Steinmetz, M.O. (1998). An autonomous folding unit mediates the assembly of two-stranded coiled coils. Proc. Natl. Acad. Sci. USA *95*, 13419–13424.

Kohn, W.D., Kay, C.M., and Hodges, R.S. (1998). Orientation, positional, additivity, and oligomerization-state effects of interhelical ion pairs in α-helical coiled-coils. J. Mol. Biol. *283*, 993–1012.

Konigsberg, W.H., and Henderson, L. (1983). Removal of sodium dodecyl-sulfate from proteins by ion-pair extraction. Methods Enzymol. *91*, 254–259.

Krylov, D., Mikhailenko, I., and Vinson, C. (1994). A thermodynamic scale for leucine zipper stability and dimerization specificity: e and g interhelical interactions. EMBO J. *13*, 2849–2861.

Lavigne, K.J., and Kim, P.S. (1995). Measurement of interhelical electrostatic interactions in the GCN4 leucine zipper. Science *268*, 1137–1138.

Letai, A., and Fuchs, E. (1995). The importance of intramolecular ion pairing in intermediate filaments. Proc. Natl. Acad. Sci. USA *92*, 92–96.

Lumb, K.J., and Kim, P.S. (1995). Measurement of interhelical electrostatic interactions in the GCN4 leucine zipper. Science *268*, 436–439.

North, A.C.T., Steinert, P.M., and Parry, D.A.D. (1994). Coiled-coil stutter and link segments in keratin and other intermediate filament molecules. Proteins *20*, 174–184.

O'Shea, E.K., Klemm, J.D., Kim, P.S., and Alber, T. (1993a). X-ray structure of the GCN4 leucine zipper, a two-stranded parallel coiled-coil. Science *254*, 539–544.

O'Shea, E.K., Limb, K.J., and Kim, P.S. (1993b). Peptide "Velcro": design of a heterodimeric coiled-coil. Curr. Biol. *3*, 658–667.

O'Shea, E.K., Rutkowski, R., and Kim, P.S. (1992). Mechanism of specificity in the Fos-Jun oncoprotein heterodimer. Cell *68*, 699–708.

Parry, D.A.D., and Steinert, P.M. (1995). The Structure and Function of Intermediate Filaments, Austin, TX: E Landis.

Parry, D.A.D., and Steinert, P.M. (1999). Intermediate filaments: molecular architecture, dynamics, assembly and polymorphism. Q. Rev. Biophys. *32*, 99–187.

Steinert, P.M. (1991). Organization of coiled-coil molecules in native keratin 1/keratin 10 intermediate filaments: evidence for alternating rows of antiparallel in-register and antiparallel staggered molecules. J. Struct. Biol. *107*, 157–174.

Steinert, P.M., Idler, W.W., and Zimmerman, S.B. (1976). Self-assembly of bovine epidermal keratin filaments in vitro. J. Mol. Biol. *108*, 547–567.

Steinert, P.M., Marekov, L.N., Fraser, R.D.B., and Parry, D.A.D. (1993a). Keratin intermediate filament structure: crosslinking studies yield quantitative information on molecular dimensions and mechanism of assembly. J. Mol. Biol. *230*, 436–452.

Steinert, P.M., Marekov, L.N., and Parry, D.A.D. (1993b). Conservation of the structure of keratin intermediate filaments: molecular mechanism by which different keratin molecules integrate into preexisting keratin intermediate filaments during differentiation. Biochemistry *32*, 10046–10056.

Steinert, P.M., Marekov, L.N., and Parry, D.A.D. (1993c). Diversity of intermediate filament structure: evidence that the alignment of molecules in vimentin is different from keratin intermediate filaments. J. Biol. Chem. *268*, 24916–24925.

Steinert, P.M., Marekov, L.N., and Parry, D.A.D. (1999). Molecular parameters of type IV α-internexin and type IV-type III α-internexin-vimentin copolymer intermediate filaments. J. Biol. Chem. *274*, 1657–1668.

Steinmetz, M.O., Stock, A., Schulthess, T., Landwehr, R., Lustig, A., Faix, J., Gerisch, G., Aebi, U., and Kammerer, R.A. (1998). A distinct

14 residue site triggers coiled-coil formation in cortexillin I. EMBO J. *17*, 1883–1891.

Strelkov, S.V., Herrmann, H., Geisler, N., Steinert, P.M., Aebi, U., and Burkhard, P. (1999). Toward an atomic model of intermediate filament (IF) architecture. Mol. Biol. Cell *10*, 13a (Abstract).

Wawersik, M., Paladini, R.D., Noensie, E., and Coulombe, P.A. (1997). A proline residue in the alpha-helical rod domain of type I keratin 16 destabilizes keratin heterotetramers. J. Biol. Chem. *272*, 32557–32565.

Yang, J.-M., Nam, K., Kim, H.-C., Lee, J.-H., Park, J.-K., Wu, K., Lee, E.S., and Steinert, P.M. (1999). A novel glutamic acid to aspartic acid mutation near the end of the 2B rod domain in the keratin 1 chain in epidermolytic hyperkeratosis. J. Invest. Dermatol. *112*, 376–379.

Yoon, M., Moir, R.D., Prahlad, V., and Goldman, R.D. (1998). Motile properties of vimentin intermediate filament networks in living cells. J. Cell Biol. *143*, 147–157.

Yu, Y., Monera, O.D., Hodges, R.S., and Privalov, P.L. (1996). Ion pairs significantly stabilize coiled-coils in the absence of electrolyte. J. Mol. Biol. *255*, 367–372.

Zhou, N.E., Kay, C.M., and Hodges, R.S. (1994). The net energetic contribution of interhelical electrostatic interactions to coiled-coil stability. Protein Eng. *7*, 1365–1372.